れは逆に欲する機能と立体構造を有したアミノ酸配列のデザインを可能とするだけでなく，このアミノ酸配列が有する立体構造やその機能を模倣した有機化合物の合理的設計をも可能とする．このようなバイオインフォマティクスをシステムアップするためには，未知蛋白質の機能解明や立体構造解析に加え，種々の蛋白質について膨大な多様性を有する構造変異体を網羅的に作製し，レセプター・リガンド結合の様式，生物活性などをも含めた機能情報を集積し，立体構造との連関を追求しなければならない．この点本研究で開発した「機能性人工蛋白質の迅速かつ網羅的創製システム」は，視点を変えればわずか1週間で10^8種類以上もの多様性を有する構造変異体ライブラリを作製し，その機能情報を高速集積し得る基盤技術と言える．本観点からわれわれは現在，上述の機能性人工TNF-αを含む様々な蛋白質の構造変異体の機能評価とともに，そのX線結晶構造解析を進めており，近未来的にバイオインフォマティクスへの研究展開を図ろうとしている．

4. 新たな部位特異的バイオコンジュゲーション法の確立

主として1980年代以降，DDSを視野においた医薬品開発の分野において，生理活性蛋白質の生体内安定性を改善するために，ポリエチレングリコール（PEG）などの水溶性高分子を蛋白質に結合させた，いわゆる高分子バイオコンジュゲーションが考案されてきた.[2-4,29,30] この中でPEGによる生理活性蛋白質のバイオコンジュゲーションは特にPEGylationと呼ばれている．この蛋白質のバイオコンジュゲーションは，分子量増大による腎排泄速度の減少をもたらすだけでなく，バイオコンジュゲーションに用いた修飾高分子により蛋白質の分子表面が覆われるために，プロテアーゼからの攻撃が立体障害的にブロックされ，結果として蛋白質の生体内半減期が延長される（Fig. 4）．同様の立体障害効果によって，免疫応答においても抗原性及び免

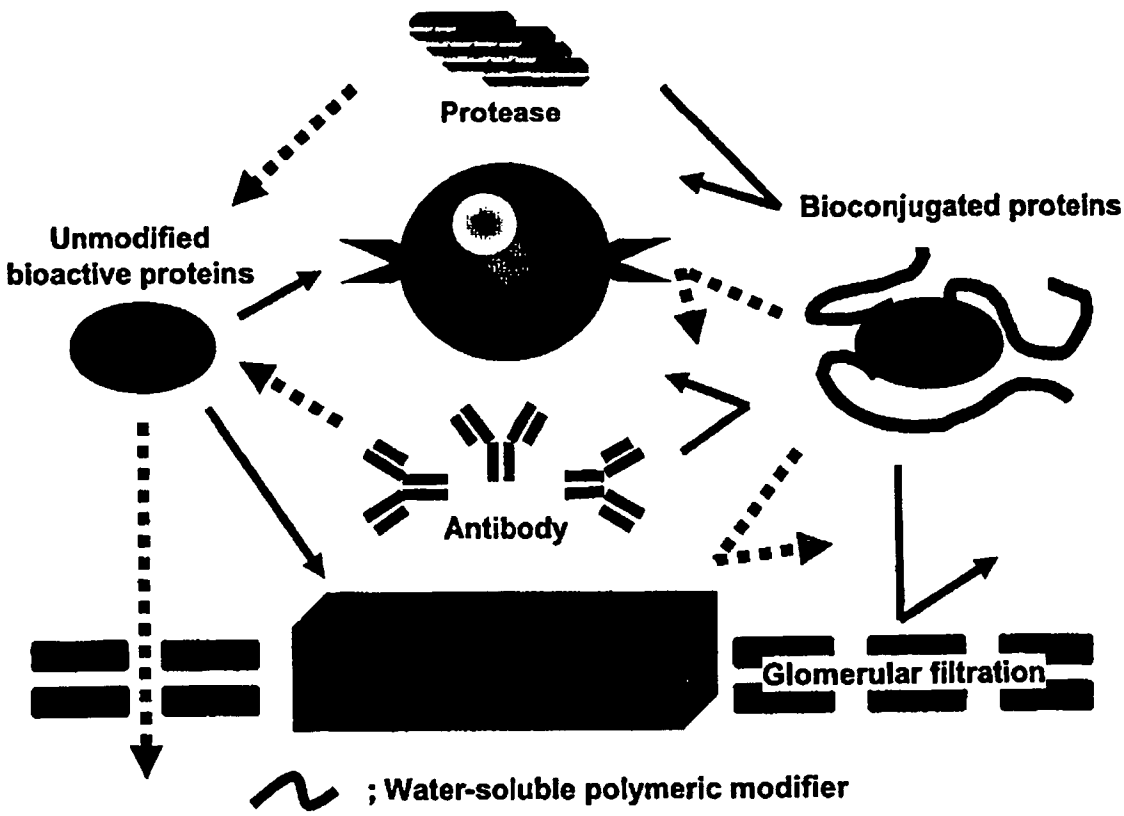

Fig. 4. Characteristics of Bioconjugated Proteins

Bioconjugated proteins with water-soluble polymeric modifiers increase their molecular size and steric hindrance, resulting in augmented plasma half-lives and stability. The medical implication of this is that PEGylation enables the therapeutic dose and frequency to be decreased.

疫原性が低下し，体内クリアランスの減少に直結する．以上に述べた総合的な体内安定化効果により，最終的に蛋白質の生体への投与量・回数を削減することが可能となる．このバイオコンジュゲーションは，数あるDDSの中でも蛋白質の医薬品化に向けた最適DDSと位置付けられてきたが，その適用は最近までAdenosine DeaminaseやSuperoxide Dismutase (SOD) といった低分子物質を基質とする酵素に限局されていた．この点に関してわれわれは，バイオコンジュゲート化SODの比活性が，用いた修飾高分子の分子量とは無関係に活性発現部位に結合した修飾高分子の数，すなわち修飾率の増加によって一義的に決定されることを認めている (Fig. 3)．以上の事実は，SODのように低分子物質を基質とする酵素の場合，結合した修飾高分子が形成する立体障害の影響を受けることなく，自由に酵素-基質複合体形成が可能となることを意味している．一方で高分子レセプターとの結合により生理活性を発現するインターロイキン-6(IL-6)の場合[31]，修飾率の増大により比活性が低下し，その低下の程度は用いた修飾高分子の分子量の増大に伴って著しくなった (Fig. 5)．したがって，活性発現に高分子レセプターとの結合を要する蛋白質においては，活性発現部位への高分子導入による避け得ない活性低下のみならず，修飾高分子が形成する立体障害に起因したリガンド-レセプター複合体の形成阻害による活性低下をも，同時に考慮しなければならない．すなわちサイトカインなどのバイオコンジュゲーションは，修飾高分子が大きければ大きいほど，プロテアーゼからの攻撃を立体障害的にブロックできるが，同時にレセプター結合をも阻害してしまうため，致命的な比活性の低下を招いてしまう．さらにバイオコンジュゲーションによる分子量増大は，腎排泄速度の減少に伴う血中滞留性の向上を果たすが，これは逆に血中から組織への移行を極度に制限してしまうことになる．このように活性発現に高分子レセプターとの結合を要する生理活性蛋白質のバイオコンジュゲーションは両刃の剣となる．

これらバイオコンジュゲーションの問題点を踏まえたうえで，抗腫瘍サイトカインとして期待されているTNF-αや血小板産生促進因子としてのIL-6などをモデル生理活性蛋白質として用い，バイオコンジュゲーション法のグレードアップを図ってきた．[31-34] その結果，1) 蛋白質の作用メカニズムを考慮し，最適の修飾高分子を選択したうえで，2) 比活性-修飾率（水溶性高分子導入率)-分子サイズなどの相関を詳細に検討し，最適条件を見出すことにより，*in vitro* における比活性低下は避け得ないものの *in vivo* においては，i) 蛋白質の生体内安定性や血中滞留性を飛躍的に向上させ得ること，ii) その生体内挙動（組織移行性）を制御し得ること，iii) 多様な *in vivo* 作用の中から，目的とする治療

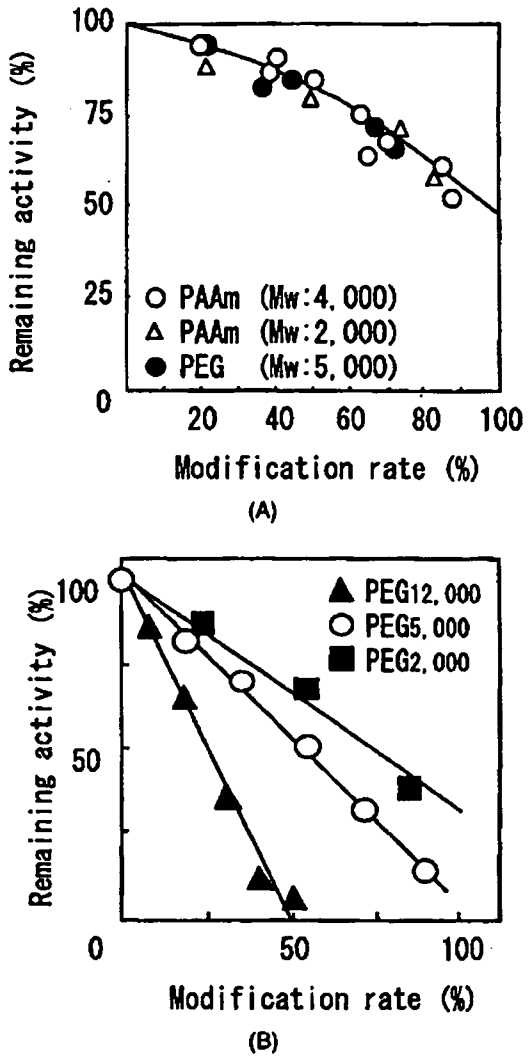

Fig. 5. Relationship between Remaining Activity and Modification Rate

A) The activity of bioconjugated SOD is independent of the molecular weight of polymeric modifier, but is proportional to the number of chemical modifications to active sites. PAAm: polyacrylamide, PEG: polyethylene glycol. B) The loss of activity of bioconjugated IL-6 is affected by both the modification rate and the molecular weight of the polymeric modifier.

作用と副作用の原因となる作用を選択分離し，目的作用のみを数百倍にも高め得ることを明らかにした．この iii) の生理活性蛋白質への作用の選択性付与は，体内安定性の向上に伴う投与量の削減や副作用発現組織への移行性低下によることを見出しており，例えばこれまでに PEG 化 TNF-α や PEG 化 IL-6 の場合，副作用を増幅することなく目的とする抗腫瘍効果や血小板産生促進効果がそれぞれ 100 倍及び 500 倍にも選択増強されることを認めている (Fig. 6)．このような背景から近年では，活性発現に高分子レセプターとの結合を要する生理活性蛋白質のバイオコンジュゲーションが世界的に試みられるようになり，最近 PEG 化インターフェロン -α が C 型肝炎に対する特効薬として上市された．

しかしながら，バイオコンジュゲーションは蛋白質に高い品質保証を付与できる最適 DDS と世界的に認識されているものの，依然としてその成功例は極めて少ない．この最大の原因は，活性発現部位への水溶性高分子導入による致命的な比活性低下と，バイオコンジュゲート化蛋白質の分子的・機能的不均一性にある．これまで汎用されてきたバイオコンジュゲーション法は，アミノ基 (リジン残基の有する ε アミノ基及び N 末端の α アミノ基) をターゲットとしたものである．この方法は，反応条件が緩和なうえ，反応効率の点で最も優れており，高い収率でバイオコンジュゲート化蛋白質が得られる．しかし，修飾高分子のアミノ基への結合はランダムであり，その結合部位を厳密に制御することはできない．周知の通り，ほとんどの蛋白質においてリジン残基は高次構造の形成やリガンド-レセプター間結合などにも必須の役割を担っている．そのため，これらリジン残基への高分子導入により，必然的に著しい比活性低下を招いてしまう．またランダムに修飾高分子が導入されるため，得られたバイオコンジュゲート体は，蛋白質の様々な部位に種々個数の修飾高分子が結合した，分子的に不均一な混合物となる．その結果，バイオコンジュゲート体は比活性や体内挙動，安定性などの機能面でもヘテロな集団となってしまう．しかし現状では，ほかに適切な蛋白質の DDS が存在しないため，このような問題点を抱えつつも，蛋白質の有効性と安全性確保の観点から，このランダムなバイオコンジュゲーションを医薬開発に適用せざるを得ない（現在 C 型肝炎の特効薬として期待されている PEG 化 IFN-α は，残存活性 10—30% のヘテロ集団であることが報告されている)．したがって，疾患プロテオミクス情報を有効活用したプロテオーム創薬を推進するためには，部位特異的に効率よく高分子導入でき，高い比活性を有するバイオコンジュゲート体を創製できる方法の確立が待望されている．

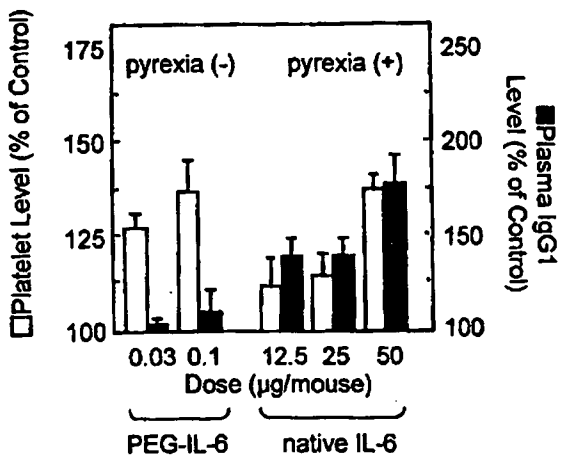

Fig. 6. PEGylation of IL-6 Effectively and Selectively Increases Its Thrombopoietic Potency

Thrombopoietic potency of PEGylated IL-6 increases more than 500-fold without compromising the incidence of undesirable side effects such as pyrexia and the introduction of antibody production.

本観点から，遺伝子工学的にシステイン残基を導入した変異蛋白質を作製し，遊離のチオール基をターゲットとした部位特異的バイオコンジュゲーション法が考案されてきた.[3] しかし一般に，フォールディングに重要な役割を担うチオール基の人為的導入は往々にして，蛋白質の立体構造変化や蛋白質間凝集を招いてしまい，予期せぬ活性低下を招いてしまう．そのうえ活性を保持したシステイン残基導入変異蛋白質が作製でき，部位特異的バイオコンジュゲーションが可能となった場合においても，チオール基への高分子導入効率の低さから，十分な収率でバイオコンジュゲート体が得られないという致命的問題を抱えている．したがって，ポストゲノム新時代の創薬テクノロジーとしてバイオコンジュゲーションをシステムアップしていくためには，アミノ基をターゲットとしたバイオコンジュゲーションと同様の良好な高分子導入効率を保ったまま，修飾部位を限局し得るテクノロジーの確立が必須となっている．

この点，前述したファージ表面提示法を駆使した「医薬価値に優れた機能性人工蛋白質を迅速創製できる蛋白質分子進化戦略」との融合アプローチにより，完全に活性を保持したリジン欠損機能性人工蛋白質を創製することによって，「*N*末端アミノ基だけを標的とした部位特異的バイオコンジュゲーション」に初めて成功した.[2] このリジン欠損機能性人工蛋白質に対する部位特異的バイオコンジュゲーションは，*N*末端アミノ基にのみ高分子導入されるため，分子的均一性に優れたバイオコンジュゲート体がほぼ100%の収率で得られる．例えばTNF-αの場合，分子内に6個（三量体として18個）のリジン残基を有しており，なかでも，Lys11は三量体形成や立体構造の維持に重要な役割を担っていることが判明している.[35] またArg32—Leu36, Ala84—Val91などの残基がサブユニットの間にまたがってクラスターを形成し，レセプター結合部位となっており，この部分に存在するLys90に加え，Lys65も活性発現に重要な役割を果たしているものと考えられている.[36,37] したがって，アミノ基に対するランダムなバイオコンジュゲーション法では，これら活性発現や構造形成に関与するリジン残基（Lys11・Lys65・Lys90）までもが修飾されてしまうため，活性低下を避け得なかった．事実，wTNF-αのアミノ基に対するランダムPEGylationでは，多様な修飾率（PEG導入率）のPEG化wTNF-αが得られてしまうが，その中から1分子のPEG導入体（ランダムモノPEG化wTNF-α; ran-PEG-TNF-α）の収率は20%程度に過ぎない．このran-PEG-TNF-αの残存活性を検討したところ，わずか1分子のPEGの導入によりwTNF-αの約10%にまで比活性が減少していた（Fig. 3）．一方で，*N*末端側の8個のアミノ酸を欠損させてもTNF-αの活性は損なわれないことから，活性発現に*N*末端側は重要でないものと考えられている.[9] そのため，*N*末端アミノ基に対する部位特異的モノPEG化リジン欠損TNF-α（sp-PEG-mTNF-α）は80%以上の活性を保持しているなど，圧倒的な利点を有していることが判明した（Fig. 1）．この分子的均一性や比活性，収率に優れた部位特異的PEG化リジン欠損TNF-αは，血中滞留性や抗腫瘍作用の選択的発現能に優れているうえ，従来法で作製したランダムPEG化TNF-αよりも著しく強い*in vivo*抗腫瘍効果を有していることも見出しており，現在臨床応用に向けた研究を推進中である．一方，*N*末端領域が活性発現に必須である蛋白質の場合でも，機能性リジン欠損体を創製したうえで，活性発現とは無関係な領域に新たなリジン残基を挿入することにより，αアミノ基とεアミノ基との反応性の違いを利用した部位特異的バイオコンジュゲーションが可能となることも判明している．以上の革新的な部位特異的バイオコンジュゲーション法は，本研究で確立した「機能性人工蛋白質の分子進化戦略」との融合により機能性リジン欠損体を創製することによって初めて可能となる．現在，種々の蛋白質に関して，活性を十二分に保持したリジン欠損体創出を進めており，今後*N*末端アミノ基への部位特異的バイオコンジュゲーションの有用性をさらに追求していく予定である．

5. DDS機能を有した機能化高分子キャリアの設計

従来より，バイオコンジュゲート化蛋白質の生体内挙動や*in vivo*薬効発現強度が，蛋白質表面を覆う修飾高分子の諸性質によって運命付けられることに着目し，バイオコンジュゲーション法のさらなるグレードアップを目的に，薬物徐放化能や標的指向能といったDDS機能を有する高分子キャリアの分子設計を図ってきた．例えば，血中滞留性の向上を目的としたバイオコンジュゲーションにはPEGよりもポリビニルピロリドン（PVP）が圧倒的に優れた修飾高分子であること，新規合成したマレイン酸導入PVPやラウリル酸導入PVPがそれぞれIFN-γ誘導能（抗腫瘍免疫誘導能）や高度な脾臓指向能を有していることなどを明らかにしてきた.[29] これら新規修飾高分子を用いたバイオコンジュゲーションは，単に蛋白質の生体内安定性を高めるだけでなく，高度な組織ターゲティング能や新たな薬理活性を導入することにより，生理活性蛋白質の目的とする治療作用の選択的発現をさらに保証することを認めている．このような一連の研究を通じて最近，腎臓への高度な薬物送達能とpH応答性薬物徐放化能を併せ持った高分子キャリア［Poly (vinylpyrrolidone-co-dimethyl maleic anhydride); PVD］を新規合成することに成功した.[4] このPVDは，pH 8以上で蛋白質のアミノ基と結合し，pH 7以下で結合蛋白質を徐々に解離する．一般に炎症組織や

癌組織では正常組織よりも低 pH であることから，PVD を薬物キャリアとして適用した場合，病態組織でのみ効果的に蛋白質が pH 応答的に徐放されることを意味している．この PVD をマウスに尾静脈内投与したところ，数時間後に投与量の約 80% が腎臓へ選択的に集積し，4 日後には 40% に減少していた (Fig. 7)．この PVD は腎尿細管上皮細胞へのみ選択的に取り込まれるが，細胞毒性を全く示さないうえ，大量投与しても腎臓を含め他の組織に何ら傷害を及ぼさない．さらに PVD でバイオコンジュゲーションした抗炎症蛋白質 (SOD) は生体内安定性に優れ，かつ静脈内投与後，選択的に腎臓へ高集積し，著しい腎炎治療作用を発揮することを見出した．高齢化社会を迎え，腎不全を初めとする腎疾患が世界的に深刻な社会問題となっている．[38] しかし慢性腎疾患に対する治療は，腎移植と透析に頼らざるを得ないのが現状であり，患者の QOL (Quality of Life) の観点からも，安全かつ有効な薬物療法の確立が待望されている．[39] 本観点から現在，上述した「医薬価値に優れた機能性人工蛋白質を迅速創製できる蛋白質分子進化戦略」による機能性人工蛋白質の創製や部位特異的バイオコンジュゲーションシステムとの融合により，新たな腎疾患治療戦略の確立をさらに推進している．

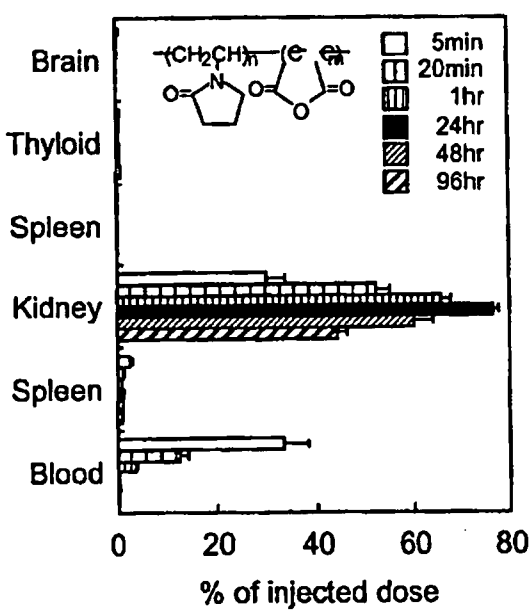

Fig. 7. Tissue Distribution of Poly (VP-co-DMMAn); PVD after *i.v.* Injection

^{125}I-labelled PVD was injected into the tail vein of BALB/c mice and tissues were collected over different periods of time post-injection (from 5 mins to 96 hrs) and the radioactivity measured by γ-counter. Each point represents the mean ±S.D.

6. おわりに

本稿で紹介した 3 段階の「プロテオーム創薬に叶う DDS 基盤テクノロジー」は，プロテオーム創薬の実現に向けて，相乗的に機能するものと期待している．一方で最近，Gene shuffling[40] や人工遺伝暗号システム[41]などを用いた機能性人工蛋白質の創出に注目が集まっている．これら興味深いアプローチは天然に存在しない新たなアミノ酸配列を有した人工蛋白質を作製しようとするものであるが，残念ながら臨床応用可能な非天然型生理活性蛋白質の創製には至っていない．当然のことながら，本研究で確立した DDS 基盤テクノロジーはこれら非天然型生理活性蛋白質の探索や創製，安定化や高機能化にも適用可能であり，現在 Gene shuffling 法とファージ表面提示法を融合した新たな機能性人工蛋白質の創出システムの構築を進めている．

また前述したように疾患プロテオミクス情報を有効活用したプロテオーム創薬を推進するためにはまず，多種多様な蛋白質とその構造変異体を網羅的に作製し，これらのレセプター・リガンド結合の様式・強度などをも含めた機能情報をハイスループットに評価可能な方法論の構築と，その立体構造との連関を網羅的に評価することが必須となる．そのうえで，ゲノムシーケンス情報を基に新たに見出された蛋白性シーズなどの機能と構造を予測し得るバイオインフォマティクスが構築されて，ようやく真の意味でプロテオーム創薬が可能となってくる．この点，ファージ表面提示法を駆使した「医薬価値に優れた機能性人工蛋白質を迅速創製できる蛋白質的分子進化戦略」は，膨大な多様性を持った構造変異体を創出し，その機能解析を迅速に大量解析し得る最適の基盤テクノロジーとなり得る．以上の研究成果は，得られた数多くの機能性人工蛋白質の立体構造と機能特性との連関評価を通じて，「機能 (医薬価値)→構造」に関する知見の集積が可能となり，将来的に機能性人工蛋白質を合理的設計し得る「プロテオーム創薬のためのバイオインフォマティクス」の構築にも貢献し得るものと期待される．

謝辞　筆者が平成 16 年度日本薬学会奨励賞を受賞できましたのは，ひとえに神戸学院大学学長・

大阪大学名誉教授の恩師　真弓忠範先生のご懇篤なるご指導，ご鞭撻の賜であり，心から厚く御礼を申し上げます．また本総説で示した筆者のこれまでの研究は，主として大阪大学薬学研究科助教授，中川晋作先生をはじめとする大阪大学薬学研究科薬剤学分野の皆様にご協力を頂きました．この場をお借りして感謝申し上げます．最後になりましたが，本研究は文部科学省科学研究費，厚生労働省科学研究費に加え，ヒューマンサイエンス振興財団や武田科学振興財団，千里ライフサイエンス振興財団のご援助を賜りました．ここに御礼を申し上げます．

REFERENCES AND NOTES

1) Present address: National Institute of Health Sciences, Osaka Branch Fundamental Research Laboratories for Development of Medicine, 7-6-8 Saito-Asagi, Ibaraki 567-0085, Japan.
2) Yamamoto Y., Tsutsumi Y., Yoshioka Y., Nishibata T., Kobayashi K., Okamoto T., Mukai Y., Shimizu T., Nakagawa S., Nagata S., Mayumi T., *Nat. Biotechnol.*, **21**, 546–552 (2003).
3) Tsutsumi Y., Onda M., Nagata S., Lee B., Kreitman R. J., *Proc. Natl. Acad. Sci. U.S.A.*, **97**, 8548–8553 (2000).
4) Kamada H., Tsutsumi Y., Sato-Kamada K., Yamamoto Y., Yoshioka Y., Okamoto T., Nakagawa S., Nagata S., *Nat. Biotechnol.*, **21**, 399–404 (2003).
5) Onda M., Nagata S., Tsutsumi Y., Vincent J. J., Wang Q., Kreitman R. J., Lee B., *Cancer Res.*, **61**, 5070–5077 (2001).
6) Smith G. P., *Science*, **228**, 1315–1317 (1985).
7) Oettgen H. F., Carswell E. A., Kassel R. L., Fiore N., Williamson B., Hoffmann M. K., Haranaka K., *Recent Results Cancer Res.*, **75**, 207–212 (1980).
8) Aggarwal B. B., Kohr W. J., Hass P. E., Moffat B., Spencer S. A., Henzel W. J., Bringman T. S., Nedwin G. E., Goeddel D. V., *J. Biol. Chem.*, **260**, 2345–2354 (1985).
9) Jones E. Y., Stuart D. I., *Nature*, **338**, 225–228 (1989).
10) Old L. J., *Science*, **230**, 630–632 (1985).
11) Sugarman B. J., Aggarwal B. B., Hass P. E., Figari I. S., Palladino Jr. M. A., Shepard H. M., *Science*, **230**, 943–945 (1985).
12) Creaven P. J., Brenner D. E., Cowens J. W., Huben R. P., Wolf R. M., Takita H., Arbuck S. G., Razack M. S., Proefrock A. D., *Cancer Chemother. Pharmacol.*, **23**, 186–191 (1989).
13) Chapman P. B., Lester T. J., Casper E. S., Gabrilove J. L., Wong G. Y., Kempin S. J., Gold P. J., Welt S., Warren R. S., Starnes H. F., *J. Clin. Oncol.*, **5**, 1942–1951 (1987).
14) Kimura K., Taguchi T., Urushizaki I., Ohno R., Abe O., Furue H., Hattori T., Ichihashi H., Inoguchi K., Majima H., *Cancer Chemother. Pharmacol.*, **20**, 223–229 (1987).
15) Spriggs D. R., Sherman M. L., Michie H., Arthur K. A., Imamura K., Wilmore D., Frei E. 3rd, Kufe D. W., *J. Natl. Cancer Inst.*, **80**, 1039–1044 (1988).
16) Yoshida J., Wakabayashi T., Mizuno M., Sugita K., Yoshida T., Hori S., Mori T., Sato T., Karashima A., Kurisu K., J. *Neurosurg.*, **77**, 78–83 (1992).
17) Taguchi T., *Gan To Kagaku Ryoho*, **13**, 3491–3497 (1986).
18) Eggermont A. M., Schraffordt Koops H., Lienard D., Kroon B. B., van Geel A. N., Hoekstra H. J., Lejeune F. J., *J. Clin. Oncol.*, **14**, 2653–2665 (1996).
19) Halme M., Maasilta P., Repo H., Leirisalo-Repo M., Taskinen E., Mattson K., Cantell K., *J. Immunother. Emphasis Tumor Immunol.*, **15**, 283–291 (1994).
20) Anasetti C., Hansen J. A., Waldmann T. A., Appelbaum F. R., Davis J., Deeg H. J., Doney K., Martin P. J., Nash R., Storb R., *Blood*, **84**, 1320–1327 (1994).
21) Vaglini M., Belli F., Santinami M., Arienti F., Parmiani G., Persiani L., Santoro N., Grazia Inglese M., D'Elia F., Cascinelli N., *Ann. Surg. Oncol.*, **2**, 61–70 (1995).
22) Debs R. J., Fuchs H. J., Philip R., Brunette E. N., Duzgunes N., Shellito J. E., Liggitt D., Patton J. R., *Cancer Res.*, **50**, 375–380 (1990).
23) Okada N., Kaneda Y., Miyamoto H., Yamamoto Y., Mizuguchi H., Tsutsumi Y., Nakagawa S., Mayumi T., *Jpn. J. Cancer Res.*, **87**, 831–836 (1996).
24) Utoguchi N., Mizuguchi H., Saeki K., Ikeda K., Tsutsumi Y., Nakagawa S., Mayumi T.,

Cancer Lett., **89**, 7–14 (1995).
25) Utoguchi N., Mizuguchi H., Dantakean A., Makimoto H., Wakai Y., Tsutsumi Y., Nakagawa S., Mayumi T., *Br. J. Cancer*, **73**, 24–28 (1996).
26) Kayton M. L., Libutti S. K., *Curr. Opin. Investig. Drugs*, **2**, 136–138 (2001).
27) Gaskill H. V. 3rd, *J. Surg. Res.*, **44**, 664–671 (1988).
28) Tsan M. F., White J. E., Santana T. A., Lee C. Y., *J. Appl. Physiol.*, **68**, 1211–1219 (1990).
29) Kamada H., Tsutsumi Y., Yamamoto Y., Kihira T., Kaneda Y., Mu Y., Kodaira H., Tsunoda S. I., Nakagawa S., Mayumi T., *Cancer Res.*, **60**, 6416–6420 (2000).
30) Kaneda Y., Yamamoto Y., Kamada H., Tsunoda S., Tsutsumi Y., Hirano T., Mayumi T., *Cancer Res.*, **58**, 290–295 (1998).
31) Tsutsumi Y., Tsunoda S., Kamada H., Kihira T., Kaneda Y., Ohsugi Y., Mayumi T. *Thromb. Haemost.*, **77**, 168–173 (1997).
32) Tsutsumi Y., Kihira T., Tsunoda S., Kanamori T., Nakagawa S., Mayumi T., *Br. J. Cancer*, **71**, 963–968 (1995).
33) Tsutsumi Y., Tsunoda S., Kamada H., Kihira T., Nakagawa S., Kaneda Y., Kanamori T., Mayumi T., *Br. J. Cancer*, **74**, 1090–1095 (1996).
34) Tsutsumi Y., Kihira T., Tsunoda S., Kamada H., Nakagawa S., Kaneda Y., Kanamori T., Mayumi T., *J. Pharmacol. Exp. Ther.*, **278**, 1006–1011 (1996).
35) Yamagishi J., Kawashima H., Matsuo N., Ohue M., Yamayoshi M., Fukui T., Kotani H., Furuta R., Nakano K., Yamada M., *Protein Eng.*, **3**, 713–719 (1990).
36) Van Ostade X., Tavernier J., Prange T., Fiers W., *EMBO J.*, **10**, 827–836 (1991).
37) Loetscher H., Stueber D., Banner D., Mackay F., Lesslauer W., *J. Biol. Chem.*, **268**, 26350–26357 (1993).
38) Jones C. A., McQuillan G. M., Kusek J. W., Eberhardt M. S., Herman W. H., Coresh J., Salive M., Jones C. P., Agodoa L. Y., *Am. J. Kidney Dis.*, **32**, 992–999 (1998).
39) Progress and Priorities: Renal disease research plan. Peport of the strategic planning conferences-Renal research properties-sponsored by National Institute of Diabetes and Digestive and Kidney Disease, Council of American Kidney Societies, (December 5–6, 1998 & February 4–5, 1999).
40) Chang C. C., Chen T. T., Cox B. W., Dawes G. N., Stemmer W. P., Punnonen J., Patten P. A., *Nat. Biotechnol.*, **17**, 793–797 (1999).
41) Hirao I., Ohtsuki T., Fujiwara T., Mitsui T., Yokogawa T., Okuni T., Nakayama H., Takio K., Yabuki T., Kigawa T., Kodama K., Nishikawa K., Yokoyama S., *Nat. Biotechnol.*, **20**, 177–182 (2002).

Available online at www.sciencedirect.com
SCIENCE DIRECT®
Biomaterials 25 (2004) 3259–3266
Biomaterials
www.elsevier.com/locate/biomaterials

The use of PVP as a polymeric carrier to improve the plasma half-life of drugs

Yoshihisa Kaneda[1], Yasuo Tsutsumi*[,1], Yasuo Yoshioka[1], Haruhiko Kamada, Yoko Yamamoto, Hiroshi Kodaira, Shin-ichi Tsunoda, Takayuki Okamoto, Yohei Mukai, Hiroko Shibata, Shinsaku Nakagawa, Tadanori Mayumi

Department of Biopharmaceutics, Graduate School of Pharmaceutical Sciences, Osaka University, 1-6 Yamadaoka, Suita, Osaka 565-0871, Japan

Received 24 June 2003; accepted 29 September 2003

Abstract

To achieve an optimum drug delivery such as targeting or controlled release utilizing bioconjugation with polymeric modifier, the conjugate between drugs and polymeric modifiers must be designed to show desirable pharmacokinetic characteristics in vivo. In this study, we assessed the biopharmaceutical properties of various nonionic water-soluble polymers as polymeric drug carriers. Polyvinylpyrrolidone (PVP) showed the longest mean resident time (MRT) after i.v. injection of all nonionic polymers with the same molecular size. In fact, tumor necrosis factor-α (TNF-α) bioconjugated with PVP (PVP-TNF-α) circulated longer than TNF-α bioconjugated with polyethylene glycol (PEG-TNF-α) with the same molecular size. Each nonionic polymeric modifier showed a different tissue distribution. Dextran was accumulated in the spleen and liver. Polydimethylacrylamide (PDAAm) tended to distribute in the kidney. However, PVP showed the minimum volume of tissue distribution. These results suggested that PVP is the most suitable polymeric modifier for prolonging the circulation lifetime of a drug and localizing the conjugated drug in blood.

Keywords: Polyethylene glycol (PEG); Polyvinylpyrrolidone (PVP); Bioconjugation; Tumor necrosis factor-alpha (TNF-α); Polymeric modifier

1. Introduction

In this post-genome era, the focus on life science research has shifted from genome analyses to genetic and protein function analyses, and recent advances in pharmacoproteomics have been drastic. Due to recent advances in structural genomics, the functions of numerous proteins will be clarified. Thus, the therapeutic application of bioactive proteins, such as newly identified proteins and cytokines, has been highly expected [1–4]. However, most of these proteins are limited in their clinical application because of unexpectedly low therapeutic effects. The reason for this limitation is that these proteins are immediately decomposed by various proteases in vivo, and are rapidly excreted from the blood circulation. Therefore, frequent administration at an excessively high dose is required to reveal their therapeutic effects in vivo. As a result, homeostasis is destroyed, and unexpected side effects occur. Many cancer chemotherapies utilizing anticancer antibiotics are also limited by such problems. Therefore, in order to overcome the weak points peculiar to many proteins, we attempted to perform chemical modification (bioconjugation) with water-soluble polymers [5–9]. Bioconjugation with polymeric modifiers improves the plasma clearance and body distribution, resulting in an increase of therapeutic effects and a decrease of side effects. Our results suggest that investigation of the relationship between degree of modification by polymer, molecular size, and specific activity on cytokine bioconjugation may accomplish an increase of therapeutic effect and a decrease of side effects. In addition, our previous study indicates that optimally bioconjugated drugs can achieve well-balanced tissue transport, receptor binding, and plasma clearance, resulting in a selective increase of therapeutic effects.

On the other hand, in order to deliver a bioconjugated drug to targeted tissue, the conjugate must be designed to show desirable pharmacokinetic characteristics, such

*Corresponding author. Tel.: +81-66879-8178; fax: +81-66879-8178.
E-mail address: tsutsumi@phs.osaka-u.ac.jp (Y. Tsutsumi).
[1]These authors contributed equally to the work.

0142-9612/$ - see front matter © 2003 Elsevier Ltd. All rights reserved.
doi:10.1016/j.biomaterials.2003.10.003

as plasma clearance and tissue distribution. It is well known that the fate and distribution of the conjugates can be attributed to the physicochemical properties of polymeric modifiers, such as molecular weight, electric charge, and hydrophilic–lipophilic balance [10]. The increase of therapeutic effects of drug bioconjugated with polymeric modifier is attributed to the pharmacokinetics of bioconjugated drug. Therefore, selecting the polymeric modifier by considering the influence of physicochemical characteristics on pharmacokinetics of polymeric modifier is markedly important. As mentioned above, sequential and multiple strategies are needed for optimization of drug therapy based on bioconjugation: (i) optimum selection of polymeric modifier considering the disposition of drugs and objectives such as targeting or controlled release; (ii) bioconjugation based on estimation of characterization, such as molecular size, modification site, degree of modification, and specific activity; and (iii) assessment of therapeutic effect and pharmacokinetics of bioconjugated drug.

In the present study, we first focused on nonionic water-soluble polymers and tried to clarify the pharmacokinetic properties of various polymeric modifiers, which could be modified by the physicochemical property, on mice bearing solid tumors. The polymer formulations used to evaluate these are PEG, polyvinylpyrrolidone (PVP), polyacrylamide (PAAm), polydimethylacrylamide (PDAAm), polyvinyl alcohol (PVA), and dextran. PVP, PAAm, and PDAAm could be functionalized by introduction of various comonomers on radical polymerization. PVA and dextran have many primary OH groups that can be used for bioconjugation on the side chain. Each ^{125}I-labeled water-soluble polymer was injected i.v. into tumor-bearing mice, and plasma clearance in the circulation and tissue distribution were measured. Moreover, we assessed the feasibility of polymeric modifiers for drug delivery based on pharmacokinetic analysis.

2. Materials and methods

2.1. Materials

PEGs (average molecular weight: 12,000, 50,000, 70,000, 500,000), acrylamide and *N*,*N*′-dimethylacrylamide, sodium pyrosulfate, chloramine T (sodium *p*-toluenesulfonchloramide trihydrate), thyramine hydrochloride, *N*,*N*′-carbonyldiimidazole, dicyclohexylcarbodiimide, *N*-vinyl-2-pyrrolidone, and *N*-hydroxysuccinimide were purchased from Wako Pure Chemical Industries, Ltd., Osaka, Japan. Methoxypolyethylene glycol-succinimidyl succinate (average molecular weight: 5000) and dextran (average molecular weight: 10,400) were obtained from Sigma Chemical Co., St. Louis, MO. PVA (80% hydrolyzed, average molecular weight: 9000–10,000) and 4,4′-azobis-(4-cyanovaleric acid) (ACVA) were purchased from Aldrich Chemical Company, Inc., Milwaukee, WI. Gel filtration chromatography (GFC) was performed by TSKgel G4000PW and TSKgel-3000 columns purchased from Tosoh Corporation, Tokyo, Japan. Econo-Pac® 10 DG columns were purchased from Bio-rad Laboratories, Hercules CA, USA. 1-Ethyl-3-(3-dimethylaminopropyl)carbodiimide hydrochloride (water-soluble carbodiimide; WSC) and β-mercaptopropionic acid (β-MP) were purchased from Dojindo Laboratories, Kumamoto, Japan. Na^{125}I (3.7 GBq/ml) solution and radioiodination system for lactoperoxidase method was purchased from NEN Research Products, Boston, MA, USA. All other chemicals were commercial reagent-grade products. Natural human tumor necrosis factor-alpha (TNF-α) was generously provided by Hayashibara Biological Laboratories, Okayama, Japan.

2.2. Animals and cells

Male ddY mice (5 weeks old) and female Balb/c mice (5 weeks old) were obtained from SLC, Hamamatsu, Japan. Sarcoma-180 (S-180) was provided from Cancer Cell Repository (CCR), Institute of Development, Aging and Cancer, Tohoku University. Meth-A cells were generously provided by Mochida pharmaceutical Co., Ltd. S-180 cells and Meth-A fibrosarcoma cells were maintained by intraperitoneal injection of cells obtained from ascitic fluid in ddY mice and Balb/c mice respectively.

2.3. Synthesis and purification of water-soluble polymers

PVP was synthesized by the radical polymerization method using ACVA and β-MP as a radical initiator and a chain transfer agent, respectively. *N*-vinylpyrrolidone, ACVA, and β-MP were added to dry *N*,*N*′-dimethylformamide (DMF). The reaction was initiated by incubation at 60°C. After incubation for 6 h, PVP was extracted in diethyl ether. The extracted PVP was dialyzed by distilled water to remove the nonreacted monomer, initiator, and chain transfer agent. PAAm and PDAAm were synthesized in dry methanol. Radical polymerization, extraction and dialysis were carried out as for PVP. PVA, dextran, and the water-soluble polymers synthesized in this study were separated into fractions by GFC in order to obtain a polymer with a narrow molecular-weight distribution. In addition, the number-average molecular weight of each fraction was calculated by comparison with PEG standards, and the same fraction of each polymer (number-average molecular weight: 5000, molecular weight dispersity < 1.14) was used.

2.4. Preparation of ^{125}I-labeled polymers

Radiolabeled polymeric modifiers were prepared by the chloramine-T method. PEGs (average molecular weight: 12,000, 50,000, 70,000, 500,000), PVA, and dextran dissolved in 1,4-dioxan were reacted with *N*,*N*′-carbonyldiimidazole for 6 h at room temperature. After dialysis in water, the activated polymers were reacted with a two-fold molar excess of thyramine hydrochloride for 48 h at 4°C. The reaction mixture was dialyzed in water and lyophilized. PAAm and PDAAm were activated with WSC, and reacted with an excessive amount of thyramine hydrochloride for 24 h at 4°C. PVP dissolved in DMF was activated with dicyclohexylcarbodiimide and *N*-hydroxysuccinimide, and reacted with an excessive amount of thyramine hydrochloride for 24 h at 4°C. Methoxypolyethylene glycol-succinimidyl succinate (average molecular weight: 5000) was also reacted with an excessive amount of thyramine hydrochloride for 24 h at 4°C. These reaction mixtures were also dialyzed in water and lyophilized. Polymer-thyramine conjugates dissolved in 0.4 M sodium phosphate buffer (2.5 mg/ml) and Na^{125}I (100 mCi/ml) were mixed in a microcentrifuge tube on ice. The labeling reaction was started by the addition of 3.8 mM chloramine-T. After iodination, the reaction was stopped by the addition of 2.5 mM sodium pyrosulfate. ^{125}I-labeled polymer was purified by GFC on the Econo-Pac® 10 DG column.

2.5. Measurement of plasma clearance and body distribution of ^{125}I-labeled polymer

S-180 cells were implanted intradermally (5×10^5/200 μl/site) into mice. On day 7, when the length of the tumors exceeded 7 mm, the mice were used for experiments. Mice bearing S-180 solid tumors were intravenously injected with ^{125}I-labeled polymer (1×10^6 cpm/200 μl). After injection, blood was collected from the tail vein at indicated times and the radioactivity was measured by a γ-counter. By rechromatographic analysis, we found that almost all the plasma ^{125}I-radioactivity at 3 h after i.v. injection was derived from intact ^{125}I-labeled polymers, but not free ^{125}I. To estimate the tissue distribution, mice were housed in metabolic cages to collect urine and sacrificed 3 h after i.v. injection. Each organ was collected, and the radioactivity was counted. The tissue distribution was expressed by the ratio of tissue radioactivity (tissue-cpm/tissue-mg) to blood radioactivity (blood-cpm/blood-mg). The pharmacokinetic parameters of each polymer were evaluated by curve fitting by means of the nonlinear least-squares program (MULTI) [11]. The peripheral distribution volume (Vd_2), the elimination constant from the central compartment (k_e), total clearance (CL_{tot}), and mean residence time (MRT) were calculated.

2.6. Synthesis of PEG-TNF-α and PVP-TNF-α

Natural human TNF-α in phosphate-buffered saline was allowed to react with a 60-fold molar excess of methoxypolyethylene glycol-succinimidyl succinate at room temperature for 10 min. The reaction was stopped by the addition of five-fold molar excess of ε-amino-n-caproic acid. PEG-TNF-α was separated into several fractions by GFC. PVP-TNF-α was also synthesized and separated in the same way. The number-average molecular weight of native TNF-α, PEG-TNF-α and PVP-TNF-α was estimated by GFC analysis by comparison with protein standards. In order to measure the elimination profile of PEG-TNF-α and PVP-TNF-α in blood, the conjugates with same molecular size (100,000–110,000) were used.

2.7. Measurement of plasma clearance of PEG-TNF-α and PVP-TNF-α

Native TNF-α, PEG-TNF-α and PVP-TNF-α were radiolabeled with ^{125}I by the lactoperoxidase method. The preparation of ^{125}I-labeled PEG-TNF-α was as described elsewhere [12]. PVP-TNF-α was also ^{125}I-labeled in the same way. The biological activities of ^{125}I-labeled native TNF-α, ^{125}I-PEG-TNF-α and ^{125}I-PVP-TNF-α were indistinguishable from those of nonradiolabeled native TNF-α, PEG-TNF-α and PVP-TNF-α, respectively. Meth-A fibrosarcoma cells (4×10^5 cells/mouse) were implanted intradermally into female Balb/c mice. On day 7, when the length of the tumors exceeded 7 mm, the pharmacokinetics of native TNF-α, PEG-TNF-α and PVP-TNF-α were studied. After i.v. injection, blood was collected from the tail vein at indicated times and the radioactivity was measured by a γ-counter. We confirmed that ^{125}I radioactivities in blood were derived from ^{125}I-labeled native TNF-α, ^{125}I-PEG-TNF-α and ^{125}I-PVP-TNF-α by GFC analysis.

3. Results

3.1. Plasma clearance of PEG with various molecular weights

We first compared the plasma clearance of PEGs with various molecular weights (Fig. 1). Elimination profiles of PEGs from the blood circulation varied to a great extent with a change of molecular weight. PEG_{5000} was most rapidly cleared from the circulation; only about 10% of the injected dose remained 20 min after i.v. administration. $PEG_{12,000}$ was retained in the blood circulation for a longer period than PEG_{5000}, but 70% of the injected dose was eliminated after 90 min. In addition, similar elimination profiles were observed for

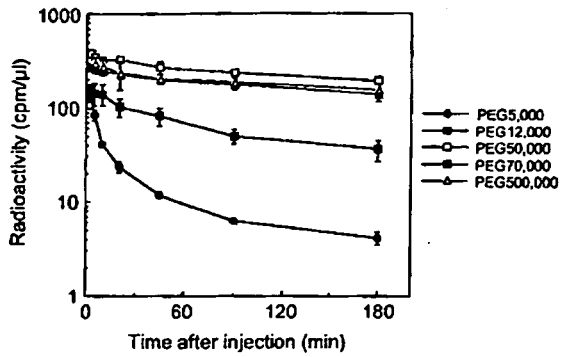

Fig. 1. Plasma clearance of PEGs with various molecular weights in mice bearing S-180 solid tumors after i.v. injection. Mice were intravenously injected with ^{125}I-labeled polymer. After administration, blood was collected from the tail vein at indicated times and the radioactivity was measured by a γ-counter. Mice were used in groups of five. Each value is mean ±SD.

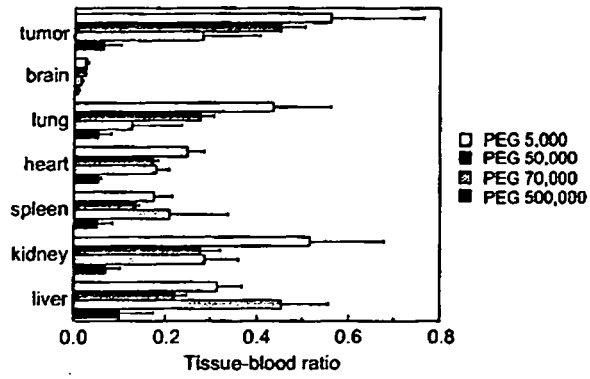

Fig. 2. Tissue distribution of PEGs with various molecular weights in mice bearing S-180 solid tumors after i.v. injection. At 3 h after i.v. injection, mice were sacrificed and each organ was collected. The radioactivity was counted by a γ-counter. Tissue distribution was expressed by the ratio of tissue radioactivity (tissue-cpm/tissue-mg) to blood radioactivity (blood-cpm/blood-mg). Mice were used in groups of five. Each value is mean ±SD.

PEGs with molecular weights of more than 50,000. These polymers circulated in blood for a long time.

3.2. Tissue distribution of PEG with various molecular weights

Fig. 2 shows the tissue distribution of PEGs with various molecular weights. The tissue distribution of PEG was suppressed by increasing the molecular weight. In particular, $PEG_{500,000}$ hardly exhibits a tissue distribution. Transport to the brain was extremely restricted for all PEGs. However, a higher polymer distribution in tumors was observed with a molecular weight of less than 50,000. Additionally, $PEG_{70,000}$ tended to be inhibited in terms of the distribution to tumors, and $PEG_{500,000}$ was completely restricted in its transport to tumors in the same as in other tissues. Fig. 3 shows urinary recovery of PEGs with various molecular weights. $PEG_{50,000}$ and $PEG_{500,000}$ were inhibited in terms of urinary excretion, with only 10% of the injected dose being excreted.

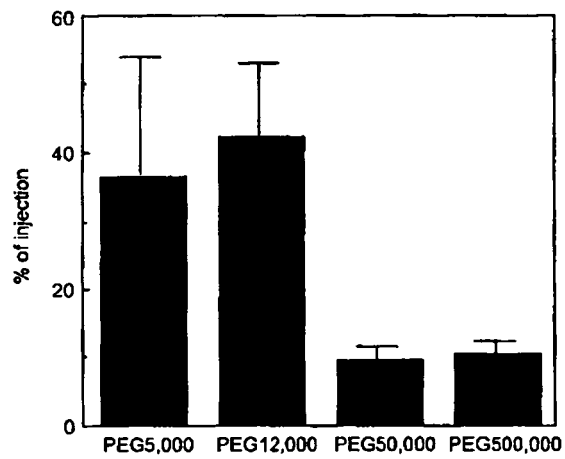

Fig. 3. Urinary excretion of PEGs with various molecular weights in mice bearing S-180 solid tumors after i.v. injection. Mice were housed in metabolic cages to collect urine for 3 h after i.v. injection. The radioactivity of urine was measured by a γ-counter. Mice were used in groups of five. Each value is mean ±SD.

3.3. Plasma clearance of various water-soluble polymers

We next studied the elimination profile of various ^{125}I-labeled polymers with the same molecular size after i.v. injection in mice bearing S-180 solid tumors. Pharmacokinetics of ^{125}I-labeled polymers was not influenced by the ^{125}I-labeling method and the preparative method of activated polymers (data not shown). Additionally, almost all radioactivities in blood were derived from ^{125}I-labeled polymers by GFC analysis 3 h after i.v. injection (data not shown). Therefore, it was considered that pharmacokinetics of ^{125}I-labeled polymers was exactly correlative to that of polymers. Fig. 4 illustrates the plasma clearance of various polymers. All polymers showed biphasic elimination patterns. PEG_{5000} and dextran, which are used frequently as drug carriers, were eliminated rapidly from the blood circulation. PDAAm, which has many methyl groups on the side chain of polymer, showed plasma clearance similar to that of PAAm. On the other hand, PVA and PVP circulated longer than the other polymers, while these nonionic polymers had the same molecular size as that of PEG_{5000}. PVP exhibited the longest residence of all the polymers in this study, and 25% of the injected dose remained after 180 min.

Table 1 summarizes the pharmacokinetic parameters of various water-soluble polymers with the same molecular size. Pharmacokinetic analysis revealed

definite differences among each polymer with respect to plasma clearance and tissue distribution. PVP showed the longest MRT of all polymers examined. The total clearance of PVP was about nine-fold lower than that of PEG_{5000}. The distribution volume of dextran was the highest of all these polymers; its volume was 3.4-fold that of PVP. PDAAm showed a higher distribution volume than PAAm. PEG also exhibited a higher distribution volume.

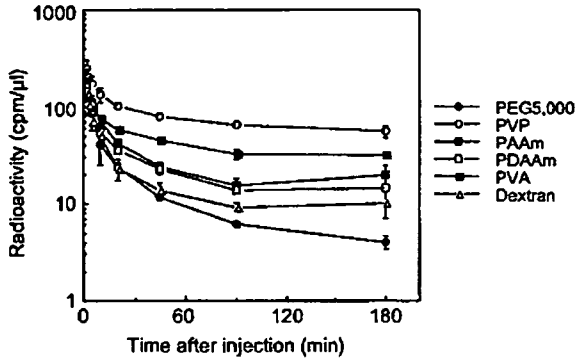

Fig. 4. Plasma clearance of various water-soluble polymers in mice bearing S-180 solid tumors after i.v. injection. Mice were intravenously injected with ^{125}I-labeled polymer. After administration, blood was collected from the tail vein at indicated times and the radioactivity was measured by a γ-counter. Mice were used in groups of five. Each value is mean±SD.

3.4. Tissue distribution of various water-soluble polymers

We next studied the tissue distribution of polymers 3 h after i.v. injection. Although all polymers with the same molecular weight dispersity in this study were nonionic and water-soluble, each polymer showed a characteristic distribution (Fig. 5). Dextran was accumulated in the liver and spleen 3 h after i.v. injection. However, PEG and PVP did not exhibit specific tissue accumulation. PVA, PAAm, and PDAAm showed an increased tendency for tissue distribution than PVP. PVA and PAAm also had no specific distribution, but PDAAm tended to accumulate in the kidney. Fig. 6 shows the urinary excretion of polymers 3 h after i.v. injection.

Table 1
Pharmacokinetic parameters of various water-soluble polymeric modifiers

	Vd_2 (μl))	k_e (min^{-1})	CL_{tot} (μl/min)	MRT (min)
$PEG_{5,000}$	18454.2±2570.3	0.068±0.004	337.2±9.8	78.9±12.4
$PEG_{12,000}$	5128.2±1539.3*	0.017±0.005*	51.7±6.2*	139.5±28.2
PVP	5920.1±193.4	0.013±0.003*	36.7±5.4*	278.8±58.3
PAAm	16833.1±3821.7	0.032±0.008	119.2±25.3*	166.3±73.6
PDAAm	13873.0±1208.5	0.055±0.002	213.1±8.9*	79.7±6.4
PVA	10199.2±991.4	0.010±0.002*	59.3±8.9*	262.5±66.4
Dextran	20034.7±3841.1	0.064±0.008	263.8±23.7	97.6±24.4

The pharmacokinetic parameters of each polymer were evaluated by curve fitting by means of the nonlinear least squares program (MULTI).
Mice were used in groups of five. Each value is the mean±S.E.
Statistical comparisons were made using the Scheffe's method after analysis of variances (ANOVA).
*$P < 0.01$, compared to $PEG_{5,000}$.

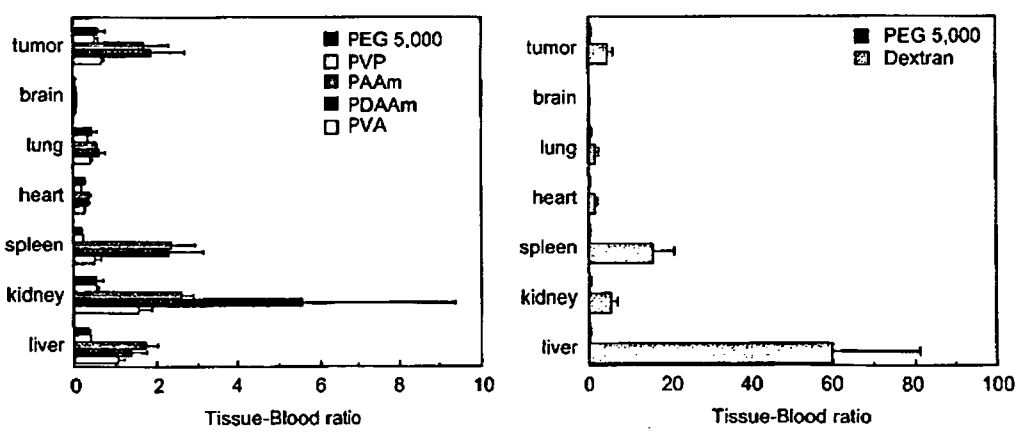

Fig. 5. Tissue distribution of various water-soluble polymers in mice bearing S-180 solid tumors after i.v. injection. At 3 h after i.v. injection, mice were sacrificed and each organ was collected. The radioactivity was counted by a γ-counter. Tissue distribution was expressed by the ratio of tissue radioactivity (tissue-cpm/tissue-mg) to blood radioactivity (blood-cpm/blood-mg). Mice were used in groups of five. Each value is mean±SD.

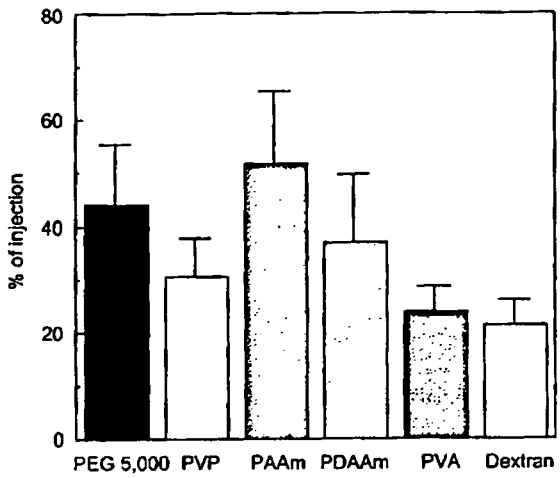

Fig. 6. Urinary excretion of various water-soluble polymers in mice bearing S-180 solid tumors after i.v. injection. Mice were housed in metabolic cages to collect urine for 3 h after i.v. injection. The radioactivity of urine was measured by a γ-counter. Mice were used in groups of five. Each value is mean ± SD.

Table 2
Pharmacokinetic parameters of bioconjugated TNF-α

	$t_{1/2}$ (min)	AUC (0–3 h) (cpm h/μl)	CL_{tot} (μl/min)	k_e ($\times 10^{-3}$/min)
Native TNF-α	4.6 ± 2.2	224 ± 44	47.2 ± 9.6	24.1 ± 8.8
PVP-TNF-α	360.1 ± 45.7	1149 ± 54	4.3 ± 0.5	2.0 ± 0.2
PEG-TNF-α	122.6 ± 85.0	1080 ± 85	3.9 ± 0.3	2.4 ± 0.2

The pharmacokinetic parameters of native and each bioconjugated TNF-α were evaluated by curve fitting by means of non-linear least squares program (MULTI).
Each value is the mean ± S.E.

Urinary recoveries of all polymers were about 20–50% of injected dose. Significant difference was not observed in all polymers examined.

3.5. *Plasma clearance of PEG-TNF-α and PVP-TNF-α*

We compared the elimination profiles of native TNF-α, PEG-TNF-α and PVP-TNF-α after i.v. injection (Table 2). Native TNF-α was rapidly cleared from the blood. However, PEG-TNF-α and PVP-TNF-α were retained in the blood for an extremely longer period than native TNF-α. In particular, PVP-TNF-α showed a slightly longer circulation lifetime than PEG-TNF-α in spite of the same molecular size.

4. Discussion

This study was aimed at clarifying the pharmacokinetic characteristics of various water-soluble polymers in order to design a bioconjugated drug and to optimize drug delivery based on bioconjugation. Additionally, we estimated the biopharmaceutical disposition of polymers in mice bearing solid tumors in consideration of cancer therapy. ^{125}I-labeled polymers showed the pharmacokinetics in mice bearing solid tumors to be the same as in normal mice (data not shown). This fundamental approach enables us to construct a rational strategy for bioconjugation not only of cytokines but also of various drugs, such as peptides and antineoplasmic agents.

PEG is a low toxic and low antigenic polymeric modifier that has been used for bioconjugation frequently. We have reported that chemical modification of TNF-α with PEG_{5000} markedly and selectively enhanced its antitumor potency when compared to native TNF-α [12]. Additionally, we assessed the relationship among the molecular weight of PEG attached to TNF-α and the degree of modification of PEG-modified TNF-α, their in vivo antitumor potency [13]. As a result, we found that PEG_{5000} is the most suitable polymeric modifier to TNF-α. This phenomenon has also been observed in PEG-modified interleukin-6 [14]. PEG, which was previously considered to be a polymeric modifier suitable for prolonging the circulation lifetime of drugs, was eliminated rapidly from the circulation (Fig. 4, Table 1). This would be mainly because urinary excretion and peripheral distribution volume (Vd_2) of PEG were relatively high (Table 1). PEG is a polyether diol of general structure $HO\text{-}(CH_2CH_2O)_n\text{-}H$, where functionalization of PEG is restricted only to the utilization of terminal primary OH groups [15]. From this viewpoint, modifiable polymeric modifiers are needed to control the biopharmaceutical characteristics of conjugated drugs. Therefore, we assessed the pharmacokinetic profile of various water-soluble polymers with molecular size of about 5000, and compared their pharmacokinetics to PEG_{5000}.

Dextran was accumulated in the liver and spleen (Fig. 5). As demonstrated clearly in Fig. 4, dextran is not appropriate for prolonging the circulation time of drugs. Polysaccharides are captured by the cells of the reticloendothelial system (RES), mainly by the liver. Therefore, it is considered that dextran is rapidly eliminated from the circulation. PVP, which can be linked with various comonomers in order to control the physicochemical properties, had the longest circulation lifetime (Fig. 4). In addition, its tissue distribution was extremely restricted (Fig. 5). The fate and distribution of conjugates between polymeric carriers and drugs can be influenced by the properties of the polymer. For example, recently, we showed polyvinylpyrrolidone-co-dimethyl maleic anhydride [poly(VP-co-DMMAn)] accumulated in the kidney (about 80% of administered dose) 24 h after intravenous injection. Additionally, conjugates between poly(VP-co-DMMAn) and

anti-inflammatoric proteins also accumulated in the kidney and accelerated recovery from acute renal failure. PVP had the longest circulation time and, its tissue distribution was extremely restricted. In addition, it is easy to introduce various comonomers on radical polymerization to PVP. These results suggest that PVP is the most feasible polymeric modifier for localizing the conjugated drug in blood. In fact, PVP-TNF-α showed a longer plasma half-life than PEG-TNF-α, and the plasma half-life of PVP-TNF-α was 90-fold higher than that of native TNF-α. As a result, PVP-TNF-α had a more potent antitumor effect than PEG-TNF-α (data not shown). Modification with polymeric modifiers such as PEG has also been used to stabilize the liposome in vivo [16] and to control the pharmacokinetics of nanoparticle carriers [17]. Therefore, PVP can be adopted not only to the bioconjugation of drugs but also to the steric stabilization of liposomes in vivo and the surface modification of particle carriers. The pharmacokinetic properties of polymers was influenced by various reasons: (1) the interaction of endothelial cells in tissues; (2) the ratio of glomerular filtration (it was influenced by the properties of polymer, such as electric charge, hydrophilic–lipophilic balance, the ability of binding to plasma proteins, and shape of polymer in blood). In dextran, we showed that dextran did not interact with bovine aortic endothelial cell (BAEC) (unpublished data). However, other researchers showed that dextran was adsorbed in rat liver parenchymal and nonparenchymal cells. Therefore, dextran may accumulate in the liver. In PEG, PVA and PAAm, we showed that these polymers did not interact with BAEC. Therefore, we considered that these polymers had long circulation time. Whereas the difference of structure was only addition of dimethyl groups, PDAAm tended to distribute in the kidney compared with PAAm. I did not have any data to explain this difference. To clarify this mechanism, we now examine the ability of PAAm to bind to endothelial cells in the kidney and renal proximal epithelial cells. PVP had the longest circulation time among polymers, and its tissue distribution was extremely restricted. It was suggested that the ability of polymer to bind to plasma protein influenced the pharmacokinetic of polymer. For example, the poly(styrene-co-maleic anhydride) (SMA) has been shown to bind to plasma albumin. SMA-conjugated neocarzinostatin (SMANCS) binds rapidly to plasma albumin when injected intravenously and showed much longer plasma half-lives. Therefore, we examined the ability of PVP to bind albumin. However, PVP did not bind to albumin. Now, we are examining the ability of PVP to bind to other plasma protein. Another idea that can explain the longer half-life of PVP is the difference of shape in blood due to the local motion of polymer. We are now examining the polymer chain dynamics in blood by computational simulation and experiment, such as the fluorescence depolarization method. On the other hand, it is well known that the permeability is very high in tumor tissue. Therefore, we studied the pharmacokinetics of polymers with various molecular sizes on the model of PEG. PEGs showed different circulation lifetimes, tissue distribution, and urinary excretion with a change of molecular weight (Figs. 1–3). These results indicate that optimum drug delivery might be achieved by considering the permeability of each organ (size barrier).

The modification of proteins and peptides by covalent attachment of polymeric modifiers can eliminate some drawbacks of native proteins and peptides and improve their physicochemical, biomedical, and pharmacological characteristics. These benefits of bioconjugation lead to the production of many chemically modified drugs, such as PEG-ADA and SMANCS, and dramatic therapeutic effects have been reported [18,19]. These approaches also exhibited that the fate and distribution of the conjugates were attributed to the physicochemical properties of polymeric modifiers. In addition, various polymeric modifiers for bioconjugation have been developed. However, with the exception of a few examples, drug therapy based on bioconjugation has not been applied for clinical use. The reason for this is that the methodology of bioconjugation has not been established for many drug therapies using antineoplasmic agents or cytokines, which needs strict control relative to targeting site and therapeutic concentration pattern. In addition, a methodology, for example, based on optimum selection of polymeric modifiers for specific characteristics of drugs and for the purpose of bioconjugation, as well as a mode of attachment, has not yet been established. Our fundamental approach will enable us to establish such a methodology of bioconjugation.

However, our approach to the molecular design of polymeric modifiers has involved only a few steps. Our previous study showed that nonionic polymers did not interact with endothelial cells, but the increase of interaction between polymers and endothelial cells is parallel to the amount of charge or hydrophobic groups (unpublished data). Therefore, we must investigate the relation between several biological factors, such as endothelial cells or plasma proteins and the physicochemical disposition, which is typified by the charge or the hydrophilic–hydrophobic balance in order to resolve the biopharmaceutical characteristics of polymeric modifiers. This approach may facilitate the optimum molecular design of polymeric modifiers in a drug delivery system.

5. Conclusion

PVP had the longest circulation lifetime among various polymers and its tissue distribution was extremely

restricted. PVP-TNF-α showed longer plasma half-life than PEG-TNF-α, and the plasma half-life of PVP-TNF-α was 90-fold higher than that of native TNF-α. These results suggest that PVP is the most suitable polymeric modifier for prolonging the circulation lifetime of a drug and localizing the conjugated drug in blood.

Acknowledgements

This study was supported in part by a Grant-in-Aid for Scientific Research (No. 15680014) from the Ministry of Education, Science and Culture of Japan, and in part by Health Sciences Research Grants for Research on Health Sciences focusing on Drug Innovation from the Japan Health Sciences Foundation (KH63124), and in part by Takeda Science Foundation.

References

[1] Furman WL, Strother D, McClain K, Bell B, Leventhal B, Pratt CB. Phase I clinical trial of recombinant human tumor necrosis factor in children with refractory solid tumors: a pediatric oncology group study. J Clin Oncol 1993;11:2205–10.

[2] Kreitman RJ, Wilson WH, Bergeron K, Raggio M, Stetler-Stevenson M, FitzGerald DJ, Pastan I. Efficacy of the anti-CD22 recombinant immunotoxin BL22 in chemotherapy-resistant hairy-cell leukemia. N Engl J Med 2001;345:241–7.

[3] Glue P, Rouzier-Panis R, Raffanel C, Sabo R, Gupta SK, Salfi M, Jacobs S, Clement RP. A dose-ranging study of pegylated interferon alfa-2b and ribavirin in chronic hepatitis C. The Hepatitis C Intervention Therapy Group. Hepatology 2000;32:647–53.

[4] Barnard DL. Pegasys (Hoffmann-La Roche). Curr Opin Invest Drug 2001;2:1530–8.

[5] Tsutsumi Y, Onda M, Nagata S, Lee B, Kreitman RJ, Pastan I. Site-specific chemical modification with polyethylene glycol of recombinant immunotoxin anti-Tac(Fv)-PE38 (LMB-2) improves antitumor activity and reduces animal toxicity and immunogenicity. Proc Natl Acad Sci USA 2000;97:8548–53.

[6] Kamada H, Tsutsumi Y, Yamamoto Y, Kihira T, Kaneda Y, Mu Y, Kodaira H, Tsunoda SI, Nakagawa S, Mayumi T. Antitumor activity of tumor necrosis factor-alpha conjugated with polyvinylpyrrolidone on solid tumors in mice. Cancer Res 2000;60:6416–20.

[7] Kaneda Y, Yamamoto Y, Kamada H, Tsunoda S, Tsutsumi Y, Hirano T, Mayumi T. Antitumor activity of tumor necrosis factor alpha conjugated with divinyl ether and maleic anhydride copolymer on solid tumors in mice. Cancer Res 1998;58:290–5.

[8] Kamada H, Tsutsumi Y, Sato-Kamada K, Yamamoto Y, Yoshioka Y, Okamoto T, Nakagawa S, Nagata S, Mayumi T. Synthesis of a poly(vinylpyrrolidone-co-dimethyl maleic anhydride) co-polymer and its application as renal targeting carrier. Nat Biotechnol 2003;21:399–404.

[9] Yamamoto Y, Tsutsumi Y, Yoshioka Y, Nishibata T, Kobayashi K, Okamoto T, Mukai Y, Shimizu T, Nakagawa S, Nagata S, Mayumi T. Site-specific PEGylation of a lysine-deficient TNF-alpha with full bioactivity. Nat Biotechnol 2003;21:546–52.

[10] Inoue M, Ebashi I, Watanabe N, Morino Y. Synthesis of a superoxide dismutase derivative that circulates bound to albumin and accumulates in tissues whose pH is decreased. Biochemistry 1989;28:6619–24.

[11] Yamaoka K, Tanigawara Y, Nakagawa T, Uno T. A pharmacokinetic analysis program (multi) for microcomputer. J Pharmacobiodyn 1981;4:879–85.

[12] Tsutsumi Y, Kihira T, Tsunoda S, Kanamori T, Nakagawa S, Mayumi T. Molecular design of hybrid tumour necrosis factor alpha with polyethylene glycol increases its anti-tumour potency. Br J Cancer 1995;71:963–8.

[13] Tsutsumi Y, Tsunoda S, Kamada H, Kihira T, Nakagawa S, Kaneda Y, Kanamori T, Mayumi T. Molecular design of hybrid tumour necrosis factor-alpha. II: The molecular size of polyethylene glycol-modified tumour necrosis factor-alpha affects its anti-tumour potency. Br J Cancer 1996;74:1090–5.

[14] Tsutsumi Y, Tsunoda S, Kamada H, Kihira T, Kaneda Y, Ohsugi Y, Mayumi T. PEGylation of interleukin-6 effectively increases its thrombopoietic potency. Thromb Haemost 1997;77:168–73.

[15] Nagasaki Y, Iijima M, Kato M, Kataoka K. Primary amino-terminal heterobifunctional poly(ethylene oxide). Facile synthesis of poly(ethylene oxide) with a primary amino group at one end and a hydroxyl group at the other end. Bioconjug Chem 1995;6:702–4.

[16] Torchilin VP, Trubetskoy VS, Whiteman KR, Caliceti P, Ferruti P, Veronese FM. New synthetic amphiphilic polymers for steric protection of liposomes in vivo. J Pharm Sci 1995;84:1049–53.

[17] Peracchia MT, Vauthier C, Puisieux F, Couvreur P. Development of sterically stabilized poly(isobutyl 2-cyanoacrylate) nanoparticles by chemical coupling of poly(ethylene glycol). J Biomed Mater Res 1997;34:317–26.

[18] Hershfield MS. PEG-ADA replacement therapy for adenosine deaminase deficiency: an update after 8.5 years. Clin Immunol Immunopathol 1995;76:S228.

[19] Konno T. Targeting chemotherapy for hepatoma: arterial administration of anticancer drugs dissolved in Lipiodol. Eur J Cancer 1992;28:403–9.

FEBS Letters 560 (2004) 178–182 FEBS 28108

RNA interfering approach for clarifying the PPARγ pathway using lentiviral vector expressing short hairpin RNA

Kazufumi Katayama[a], Koichiro Wada[b,*], Hiroyuki Miyoshi[c], Kozo Ohashi[a], Masashi Tachibana[a], Rie Furuki[a], Hiroyuki Mizuguchi[d], Takao Hayakawa[d], Atsushi Nakajima[e], Takashi Kadowaki[f], Yasuo Tsutsumi[a], Shinsaku Nakagawa[a], Yoshinori Kamisaki[b], Tadanori Mayumi[a]

[a] *Department of Biopharmaceutics, Graduate School of Pharmaceutical Science, Osaka University, Osaka 565-0871, Japan*
[b] *Department of Pharmacology, Graduate School of Dentistry, Osaka University, 1-8 Yamadaoka, Suita, Osaka 565-0871, Japan*
[c] *Subteam for Manipulation of Cell Fate, BioResource Center, RIKEN, Tsukuba Institute, Ibaraki, Japan*
[d] *Division of Biological Chemistry and Biologicals, National Institute of Health Sciences, Tokyo 158-8501, Japan*
[e] *The Third Department of Internal Medicine, Yokohama City University School of Medicine, Yokohama 236-0004, Japan*
[f] *Department of Metabolic Diseases, Graduate School of Medicine, University of Tokyo, Tokyo, 113-0033, Japan*

Received 15 December 2003; revised 10 January 2004; accepted 22 January 2004

First published online 4 February 2004

Edited by Robert Barouki

Abstract **Peroxisome proliferator-activated receptor γ(PPARγ) plays a central role in adipocyte differentiation and insulin sensitivity. Although PPARγ also appears to regulate diverse cellular processes in other cell types such as lymphocytes, the detailed mechanisms remain unclear. In this study, we established a lentivirus-mediated short hairpin RNA expression system and identified a potent short hairpin RNA which suppresses PPARγ expression, resulting in marked inhibition of preadipocyte-to-adipocyte differentiation in 3T3-L1 cells. Our PPARγ-knockdown method will serve to clarify the PPARγ pathway in various cell types in vivo and in vitro, and will facilitate the development of therapeutic applications for a variety of diseases.**

Key words: Peroxisome proliferator-activated receptor γ; RNA interference; Short hairpin RNA; Lentiviral vector; Adipocyte

1. Introduction

The peroxisome proliferator-activated receptor (PPAR) family was discovered as an orphan nuclear receptor, and three different subtypes were subsequently identified, namely PPARα, PPARδ/β and PPARγ. PPARγ is abundantly expressed in adipose tissue and plays a key role in adipocyte differentiation and insulin sensitivity [1]. Recently, our group and other researchers reported that PPARγ is also an attractive therapeutic target as it can play an important role in immune responses, especially in transcriptional regulation of inflammatory responses [2–5].

The biological role of PPARγ had been widely investigated by using PPARγ-deficient mice generated by targeted disruption of the PPARγ gene. Since homozygous PPARγ-deficient mice ($PPAR\gamma^{-/-}$) are embryonic lethal due to placental dysfunction [1], heterozygous mice ($PPAR\gamma^{+/-}$) have been used to investigate the role of PPARγ in vivo experiments. However, $PPAR\gamma^{+/-}$ mice seem to be of limited use in some experiments, because PPARγ also appears to regulate diverse cellular processes in cells that show lower levels of PPARγ expression in comparison to adipose tissue [6,7].

RNA interference (RNAi) is a powerful technique for selectively silencing the expression of genes. Recent work has provided a system for the stable expression of short interfering RNA (siRNA) in mammalian cells, which is generally based on the expression of short hairpin RNA (shRNA) under the control of the RNA polymerase III promoter [8–11]. The technique has allowed for the development of a new approach for achieving targeted gene silencing of disease-associated genes in animal models as well as in cultured cells.

Lentiviral vectors (LVs) are a promising tool for exogenous gene transfer among gene transfer vehicles, because LVs have the advantages of infecting non-dividing cells and being stably integrated into the host genome resulting in long-term expression of transgene [12–16]. Furthermore, recent reports have demonstrated that virus-mediated RNAi could provide long-term silencing in mammalian cells [9,17,18]. In the present study, we attempted to develop a technique for suppressing the expression of PPARγ in vivo and in vitro. We established a lentivirus-mediated shRNA expression system and identified a potent shRNA target sequence in the coding region of PPARγ mRNA. This approach has enabled us to clarify a novel role of PPARγ.

2. Materials and methods

2.1. Vector construction

Vectors were constructed using standard cloning procedures. H1-RNA promoter was amplified from human genomic DNA (Clontech, Palo Alto, CA, USA) using the following primers: 5′-CCATGGAATTCGAACGCTGACGTC-3′ and 5′-GCAAGCTTAGATCTGTGGTCTCATACAGAACTTATAAGATTCCC-3′. The amplified polymerase chain reaction (PCR) product was inserted into the *Eco*RI-*Bgl*II site of pHM5 [19], generating pHM5-H1. pHM5-H1 was designed to express shRNA upon the insertion of an appropriate sequence into the *Bgl*II/*Xba*I site (Fig. 1A). Oligonucleotides encoding

*Corresponding author. Fax: (81)-6-6879 2914.
E-mail address: kwada@dent.osaka-u.ac.jp (K. Wada).

Abbreviations: LV, lentiviral vector; shRNA, short hairpin RNA; MOI, multiplicity of infection; PPAR, peroxisome proliferator-activated receptor; GPDH, glycerol-3-phosphate dehydrogenase; BRL, rosiglitazone (BRL-49653)

0014-5793/04/$30.00
doi:10.1016/S0014-5793(04)00100-0

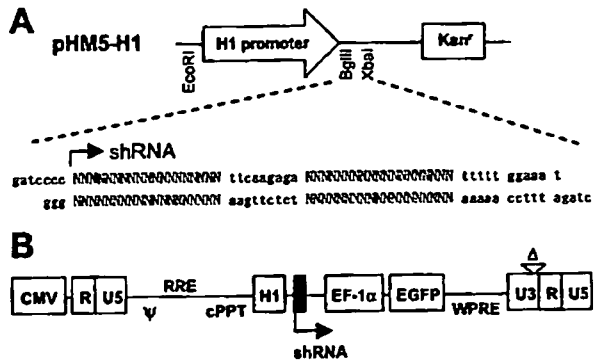

Fig. 1. Vector construction. A: pHM5-H1 was constructed as described in Section 2. Oligonucleotides encoding both strands of the targeting sequence, a spacer sequence which provided a loop structure and a transcriptional termination signal T5 were annealed and inserted into *BglII/XbaI* sites in pHM5-H1. B: Schematic representation of self-inactivating (SIN) LV plasmid (CS-H1-shRNA-EG). CMV: cytomegalovirus promoter, Ψ: packaging signal, RRE: rev responsive element, cPPT: central polypurine tract, H1: human H1 promoter, EF-1α: human elongation factor 1α subunit gene promoter, EGFP: enhanced green fluorescent protein, WPRE: woodchuck hepatitis virus posttranscriptional regulatory element. Δ: deleting 133 bp in the U3 region of the 3′ long terminal repeat.

both strands of the targeting sequence were annealed and inserted into *BglII/XbaI* sites of pHM5-H1 (Fig. 1A and Table 1). The sequence was verified on a DNA sequencer (ABI Prism 310, Applied Biosystems) and the cassette containing the H1 promoter plus the shRNA was transferred to a self-inactivating (SIN) LV construct, generating CS-H1-shRNA-EG (Fig. 1B).

2.2. Preparation of LV expressing shRNA (LV-shRNA)

LVs pseudotyped with vesicular stomatitis virus G glycoprotein (VSV-G) were prepared according to a previously described method [15,20,21]. Briefly, 293T cells were transfected with four plasmids: packaging construct (pMDLg/pRRE), VSV-G-expressing construct (pMD.G), Rev-expressing construct (pRSV-Rev), and SIN vector construct (CS-H1-shRNA-EG). Vector supernatant was concentrated by ultracentrifugation, and the pellet was resuspended in Hanks' balanced salt solution. Vector titers, which can be detected by enhanced green fluorescent protein (EGFP) expression under the control of a human elongation factor 1α subunit gene promoter, were determined by infection of HeLa P4 cells with serial dilutions of the vector stocks, followed by fluorescence-activated cell sorter (FACS) analysis for EGFP-positive cells.

2.3. Cell culture and infection of LV-shRNA

3T3-L1 preadipocytes were cultured in Dulbecco's modified Eagle's medium supplemented with 10% fetal bovine serum. The 3T3-L1 cells were infected with viral stocks at a multiplicity of infection (MOI) of 50 or 200, followed by FACS analysis for EGFP expression. Transduction efficiencies were 66.57% ± 1.44 at 50 MOI and 91.64% ± 1.07 at 200 MOI, expressed as S.E.M. The transduced 3T3-L1 cells were grown and then used in subsequent experiments.

2.4. Differentiation protocol

Induction of adipocyte differentiation was performed essentially as described [22]. Two days after confluence (day 0), the medium was replaced with differentiation medium containing rosiglitazone (BRL, 1 μM), insulin (INS, 150 nM), dexamethasone (DEX, 1 μM) and 3-isobutyl-1-methylxanthine (IBMX, 100 μM), which was changed every 3 days thereafter until analysis.

2.5. Measurement of adipocyte differentiation

Differentiation of 3T3-L1 preadipocytes to adipocytes was monitored by measurement of intracellular lipid accumulation using Oil red O staining and glycerol-3-phosphate dehydrogenase (GPDH) activity on day 9. Cultured cells were fixed for 2 h with 10% formalin in isotonic phosphate buffer and then washed with distilled water. The cells were then stained by complete immersion in a working solution (0.3%) of Oil red O for 4 h. Excess dye was removed by exhaustive washing with water. The GPDH activity was measured using a GPDH assay kit (Hokudo, Hokkaido, Japan).

2.6. RNA isolation and reverse transcription (RT) PCR analysis

Total RNA was extracted from the 3T3-L1 cells infected with each kind of LV-shRNA using Tri-Reagent (Sigma). First-strand cDNA was generated from 1 μg of RNA by using oligo(dT_{12-18}) primer (Invitrogen) and SuperScript III RNase H Reverse Transcriptase (Invitrogen) according to the manufacturer's protocol. The reverse transcription reaction mix was amplified with the following pair of oligonucleotides specific for murine PPARα, PPARδ, PPARγ2 and glyceraldehyde-3-phosphate dehydrogenase (GAPDH): PPARα, 5′-CGACAAGTGTGATCGGAGCTGCAAG-3′ and 5′-GTTGAAGTTCTTCAGGTAGGCTTC-3′; PPARδ, 5′-GGCCAACGGCAGTGGCTTCGTC-3′ and 5′-GGCTGCGGCCTTAGTACATGTCCT-3′; PPARγ2, 5′-GCTGTTATGGGTGAAACTCTG-3′ and 5′-ATAAGGTGGAGATGCAGGTTC-3′; GAPDH, 5′-GCTCACTGGCATGGCCTTC-3′ and 5′-ACCACCCTGTTGCTGTAGC-3′ [23]. The sample was amplified in the linear phase, optimized for each gene (PPARα: 38 cycles; PPARδ: 30 cycles; PPARγ2: 36 cycles; GAPDH: 23 cycles). All PCR products were electrophoresed on 2% agarose gel using 0.5× Tris-borate-EDTA buffer and visualized using ethidium bromide. The gel image was captured by a digital camera, and densitometric analysis was performed using NIH Image software.

2.7. Western blot analysis

Cultured cells were homogenized in Tris–HCl buffer containing a cocktail of protease inhibitors and insoluble materials were then removed by centrifugation at 4°C. The solubilized lysates were resolved by sodium dodecyl sulfate–polyacrylamide gel electrophoresis under reducing conditions at a concentration of 5 μg protein of sample per lane. Detection of PPARα, PPARδ, PPARγ and GAPDH was respectively performed with anti-PPARα polyclonal antibody (Santa Cruz Biotechnology, Santa Cruz, CA, USA), anti-PPARδ polyclonal antibody (Santa Cruz Biotechnology), anti-PPARγ monoclonal antibody (Santa Cruz Biotechnology) and anti-GAPDH polyclonal antibody (Trevigen, Gaithersburg, MD, USA) according to a previously described method [4]. The band intensity was quantified using NIH Image software.

2.8. Statistical analysis

All results are expressed as mean ± S.E.M. Statistical comparisons were made with Student's *t*-test or Scheffé's method after analysis of variances. The results were considered significantly different at $P < 0.05$.

Table 1
LV vectors used in this study

LV vector	shRNA target gene	shRNA target sequence
LV-shRNA-P11	PPARγ1 and 2	CAGCTCTACAACAGGCCTC
LV-shRNA-P12	PPARγ1 and 2	ATGGCCATTGAGTGCCGAG
LV-shRNA-P13	PPARγ1 and 2	TAAATGTCAGTACTGTCGG
LV-shRNA-P14	PPARγ1 and 2	TTGGCGGAGATCTCCAGTG
LV-shRNA-P15	PPARγ1 and 2	GTCTGCTGATCTGCGAGCC
LV-shRNA-P16	PPARγ1 and 2	TCACCATTTGTCATCTACG
LV-shRNA-P17	PPARγ1 and 2	GTTTGAGTTTGCTGTGAAG
LV-shRNA-P18	PPARγ1 and 2	ATGAGCCTTCACCCCCTGC
LV-shRNA-P19	PPARγ1 and 2	GATCTGCGAGCCCTGGCAA
LV-shRNA-P21	PPARγ2	ACTCTGGGAGATTCTCCTG
LV-shRNA-P22	PPARγ2	CCTTCGCTGATGCACTGCC
LV-shRNA-Lu	Luciferase	ACGCTGAGTACTTCGAAAT
LV-shRNA-Scramble	No target gene	GCGCGCTTTGTAGGATTCG
LV-EG	–	–

LV-EG has no shRNA-expressing cassette. All vectors carry an EGFP-expressing cassette as a marker gene so that the cells transduced with LV-shRNAs can be identified by green fluorescence.

3. Results and discussion

To develop an effective PPARγ-knockdown method, we constructed an LV-based siRNA system in which shRNA encoding both strands of the targeting sequence is expressed under the control of human H1 promoter [24]. A human H1 promoter was cloned to generate pHM5-H1, and oligonucleotide encoding shRNA against PPARγ mRNA was inserted (Fig. 1A). Subsequently, the cassette containing the H1 promoter plus the shRNA was transferred to the SIN LV construct (Fig. 1B). Using a shRNA target sequence against firefly luciferase, we previously demonstrated that our LV-based siRNA system effectively suppressed the target gene in mammalian cells (data not shown).

PPARγ exists as two isoforms, termed PPARγ1 and PPARγ2,

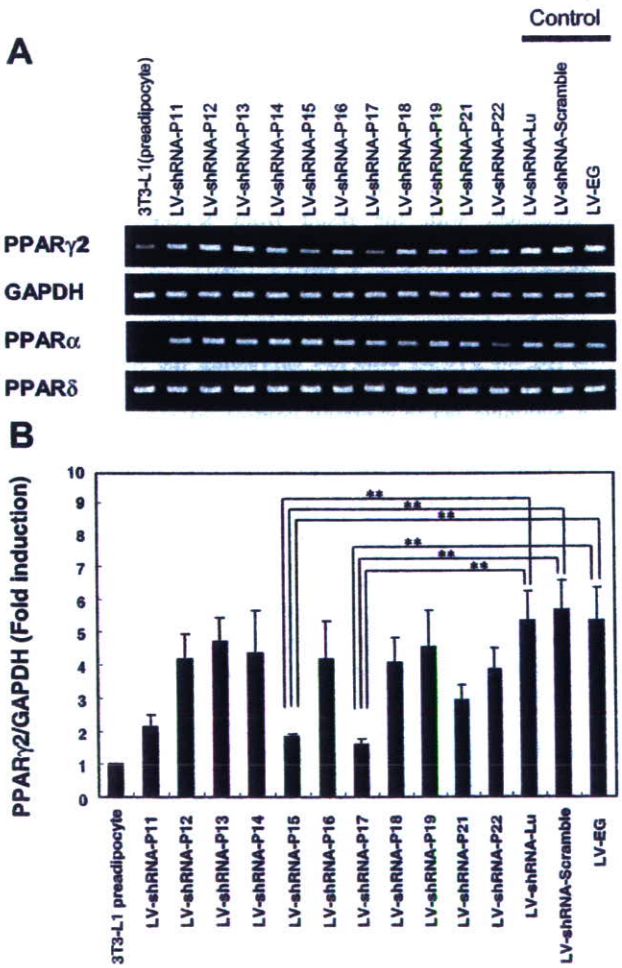

Fig. 2. Alteration of PPAR family mRNA levels in 3T3-L1 cells transduced with LV-shRNAs. A: 3T3-L1 preadipocytes were infected with each LV-shRNA (200 MOI) and then subjected to the differentiation protocol. Two days after the induction of adipocyte differentiation, mRNA levels of PPARγ2, PPARα, PPARδ, and GAPDH were determined by RT-PCR analysis. Results are representative gel images. B: Densitometric quantitation for PPARγ and GAPDH from three to four independent experiments. Each PPARγ value was normalized to the values for GAPDH and expressed as fold induction over the basal level detected in 3T3-L1 preadipocytes (bars, S.E.M.). $^{**}P < 0.01$ for LV-shRNA-P15 and -P17 compared with LV-shRNA-Lu, LV-shRNA-Scramble or LV-EG.

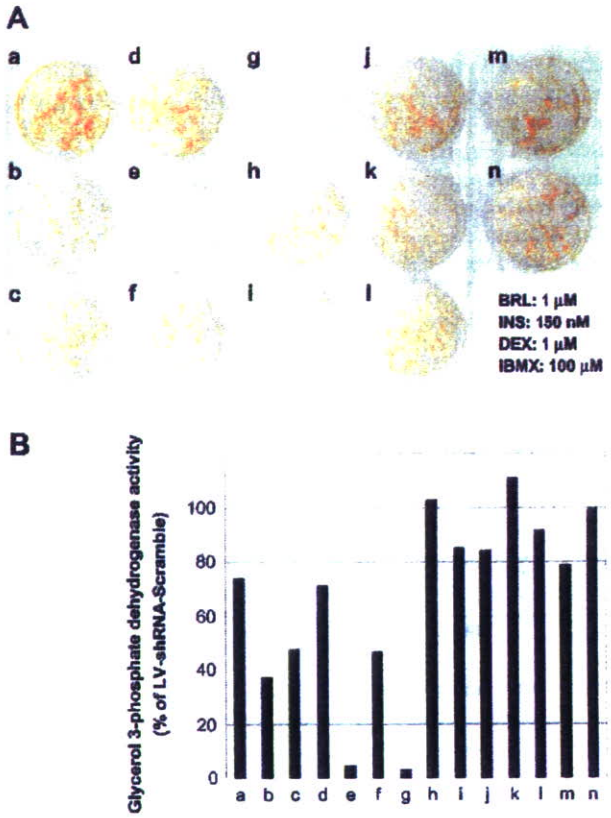

Fig. 3. Effect of LV-shRNAs on adipocyte differentiation. A: Differentiation of 3T3-L1 preadipocytes (infected with LV-shRNA; 200 MOI) to adipocytes was monitored by measurement of intracellular lipid accumulation using Oil red O staining on day 9. B: GPDH activity was measured on day 9. Data were expressed as percentage of the GPDH activity of 3T3-L1 cells which were infected with LV-shRNA-Scramble (200 MOI). a: LV-shRNA-P11; b: LV-shRNA-P12; c: LV-shRNA-P13; d: LV-shRNA-P14; e: LV-shRNA-P15; f: LV-shRNA-P16; g: LV-shRNA-P17; h: LV-shRNA-P18; i: LV-shRNA-P19; j: LV-shRNA-P21; k: LV-shRNA-P22; l: LV-EG; m: LV-shRNA-Lu; n: LV-shRNA-Scramble. Similar results were obtained in two independent experiments.

which are produced by a combination of different promoters and alternative splicing. PPARγ2 has an N-terminal extension of 30 amino acids and is very highly expressed in adipocytes [22,25]. We selected 11 target sequences in the coding region of PPARγ mRNA and constructed LV-shRNAs against PPARγ (Table 1). In the present study, LV-shRNA-Lu, LV-shRNA-Scramble and LV-EG were used as controls.

To find the most effective shRNA target sequence against PPARγ, we analyzed the silencing of PPARγ in 3T3-L1 cells during preadipocyte-to-adipocyte differentiation in which PPARγ is known to be a master regulator of adipogenesis [1,26,27]. The expression of PPARγ increases during the differentiation process and activation of PPARγ protein by its ligand leads to adipogenesis through the activation of the adipogenic gene cascade. The 3T3-L1 preadipocytes transduced with each of the LV-shRNAs, i.e. 3T3-L1 cells expressing shRNAs, as listed in Table 1, were exposed to differentiation medium (DM) 2 days after confluence (day 0). Initially, silencing of PPARγ expression was examined by RT-PCR after 2 days of culture in DM (Fig. 3). Although 3T3-L1 cells transduced with LV-shRNA-Lu, -Scramble and LV-EG showed

significant increases in the levels of PPARγ mRNA, 3T3-L1 cells transduced with LV-shRNA-P15 and -P17 retained low levels of PPARγ mRNA comparable to the level in preadipocytes maintained in normal culture medium. In contrast, the expression levels of GAPDH, PPARα and PPARδ were not altered by LV-shRNA-P15 or -P17. The other LV-shRNAs against PPARγ caused moderate decreases in the levels of PPARγ mRNA.

The differentiation of 3T3-L1 preadipocytes to adipocytes can be monitored by measurement of intracellular lipid accumulation and GPDH (an important enzyme in triglyceride synthesis) activity [28–30]. Intracellular lipid accumulation was dramatically reduced in the LV-shRNA-P15- and -P17-infected 3T3-L1 cells as shown by Oil red O staining (Fig. 3A, e: LV-shRNA-P15; g: LV-shRNA-P17). GPDH activity also demonstrated that LV-shRNA-P15 and LV-shRNA-P17 express a potent shRNA which suppresses PPARγ mRNA expression, resulting in marked inhibition of preadipocyte-to-adipocyte differentiation (Fig. 3B). We also confirmed that the expression of PPARγ-inducible genes, such as uncoupling protein-1 and adipocyte fatty acid binding protein, were inhibited in 3T3-L1 cells transduced with LV-shRNA-P15 and LV-shRNA-P17 in the presence of the PPARγ-specific ligand, BRL (unpublished data).

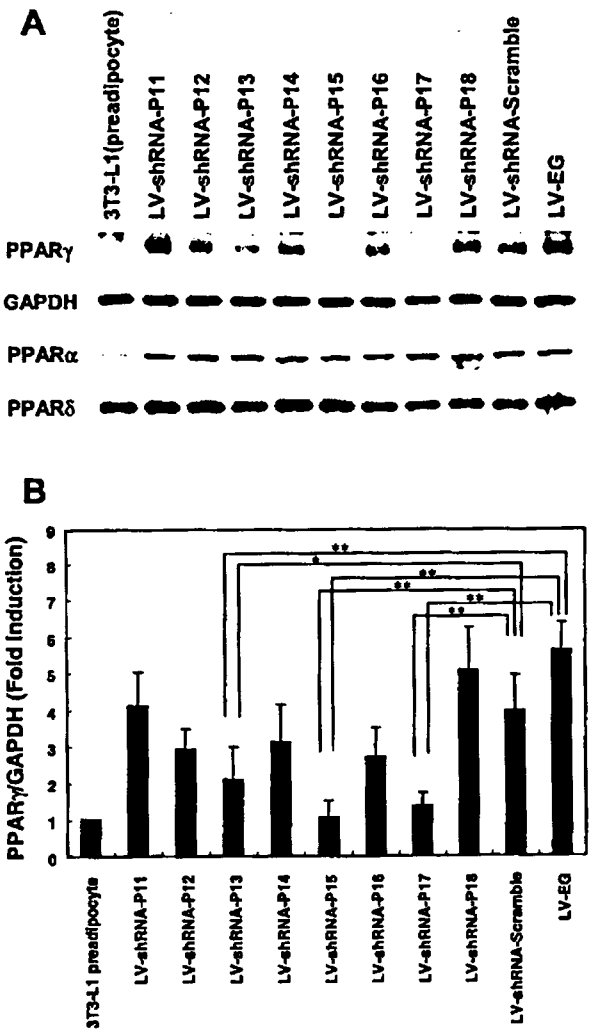

Fig. 4. Alteration of PPAR family protein levels in 3T3-L1 cells transduced with LV-shRNAs (200 MOI). A: Four days after the induction of adipocyte differentiation, the whole cell extract was analyzed by Western blotting with antibodies against PPARγ, PPARα, PPARδ and GAPDH. Results are representative of three individual experiments. B: Densitometric quantitation for PPARγ and GAPDH from three individual experiments. Each PPARγ value was normalized to the values for GAPDH and expressed as fold induction over the basal level detected in 3T3-L1 preadipocytes (bars, S.E.M.). $^{**}P<0.01$ for LV-shRNA-P13, -P15 and -P17 compared with LV-shRNA-Scramble or LV-EG. $^{*}P<0.05$ for LV-shRNA-P13 compared with LV-EG.

A recent study demonstrated that if the degree of complementarity to its target is reduced, siRNA can function as microRNAs which affect translational suppression without cleavage [31]. An important objective of this study was to determine whether the silencing effect of PPARγ caused by these LV-shRNAs was specific for PPARγ. In fact, several shRNA target sequences used in this study partially correspond to PPARα or PPARδ. Western blotting analysis demonstrated that PPARγ protein levels were significantly decreased in the LV-shRNA-P15- and LV-shRNA-P17-infected 3T3-L1 cells, while LV-shRNAs did not alter the amount of PPARα, PPARδ or GAPDH protein (Fig. 4). These results were consistent with the result from RT-PCR analysis (Fig. 2).

Furthermore, we examined 3T3-L1 cells exposed to either LV-shRNA-Scramble, -P15 or -P17 by fluorescent microscopy for EGFP expression to identify cells not infected with those vectors, i.e. the 3T3-L1 cells not expressing the shRNA encoded by LV-shRNA-P15 or -P17 (Fig. 5). In the case of LV-shRNA-Scramble, which expresses control shRNA, the differentiation of preadipocytes to adipocytes was not affected by infection with LV. In contrast, all of the cells infected with LV-shRNA-P15 or -P17 retained their fibroblast-like morphology. Taken together, these results indicate that our LV-shRNA-based PPARγ-knockdown method resulted in decreased PPARγ expression and specific inhibition of the PPARγ pathway, even in the case of adipocyte differentiation in which PPARγ expression is strongly induced by DM and PPARγ protein is effectively activated by the PPARγ-specific ligand used in this study, BRL.

Accessibility of the siRNA might depend on the secondary structure of the target mRNA. However, a clear correlation between either secondary structure or GC content and effectiveness of target sites has not yet been recognized. Although we designed 11 different shRNAs against PPARγ, we have not found any correlation between several factors that have been implicated in the accessibility of transcriptional/translational regulatory elements and effectiveness of target sites of shRNA until now.

In the present study, we developed a promising tool for suppressing the expression of PPARγ. Our PPARγ-knockdown method will serve to clarify the role of the PPARγ pathway in various cell types in vivo and in vitro, and will facilitate the development of therapeutic applications for a variety of diseases.

Acknowledgements: This work was supported in part by a grant (Tokuteiryouiki C13204072, to A.N.) from the Ministry of Education, Culture, Sports, Science and Technology, and a grant (15590227, to K.W.) from the Japan Society for the Promotion of Science.

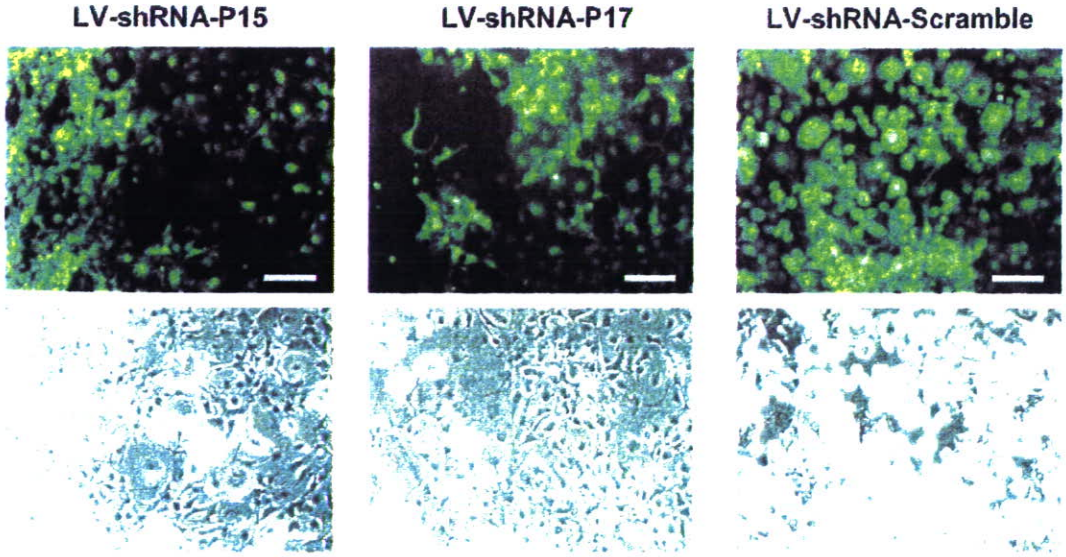

Fig. 5. Identification of the 3T3-L1 cells transduced with LV-shRNA. Brightfield and fluorescent microscopy images collected from the same field. The LV-shRNA-infected cells, which expressed EGFP, were detected as green fluorescence (upper panels) and morphologically identified mature adipocyte with a voluminous spherical shape and a large accumulation of intracytoplasmic lipid vesicles (lower panels). Bars represent 100 μm.

References

[1] Kubota, N. et al. (1999) Mol. Cell 4, 597–609.
[2] Su, C.G. et al. (1999) J. Clin. Invest. 104, 383–389.
[3] Desreumaux, P. et al. (2001) J. Exp. Med. 193, 827–838.
[4] Nakajima, A. et al. (2001) Gastroenterology 120, 460–469.
[5] Katayama, K. et al. (2003) Gastroenterology 124, 1315–1324.
[6] Schlezinger, J.J., Jensen, B.A., Mann, K.K., Ryu, H.Y. and Sherr, D.H. (2002) J. Immunol. 169, 6831–6841.
[7] Wang, Y.L., Frauwirth, K.A., Rangwala, S.M., Lazar, M.A. and Thompson, C.B. (2002) J. Biol. Chem. 277, 31781–31788.
[8] Brummelkamp, T.R., Bernards, R. and Agami, R. (2002) Science 296, 550–553.
[9] Abbas-Terki, T., Blanco-Bose, W., Deglon, N., Pralong, W. and Aebischer, P. (2002) Hum. Gene Ther. 13, 2197–2201.
[10] Hasuwa, H., Kaseda, K., Einarsdottir, T. and Okabe, M. (2002) FEBS Lett. 532, 227–230.
[11] Kunath, T., Gish, G., Lickert, H., Jones, N., Pawson, T. and Rossant, J. (2003) Nat. Biotechnol. 21, 559–561.
[12] Naldini, L., Blomer, U., Gallay, P., Ory, D., Mulligan, R., Gage, F.H., Verma, I.M. and Trono, D. (1996) Science 272, 263–267.
[13] Kafri, T., Blomer, U., Peterson, D.A., Gage, F.H. and Verma, I.M. (1997) Nat. Genet. 17, 314–317.
[14] Takahashi, M., Miyoshi, H., Verma, I.M. and Gage, F.H. (1999) J. Virol. 73, 7812–7816.
[15] Miyoshi, H., Smith, K.A., Mosier, D.E., Verma, I.M. and Torbett, B.E. (1999) Science 283, 682–686.
[16] Pfeifer, A., Kessler, T., Yang, M., Baranov, E., Kootstra, N., Cheresh, D.A., Hoffman, R.M. and Verma, I.M. (2001) Mol. Ther. 3, 319–322.
[17] Brummelkamp, T.R., Bernards, R. and Agami, R. (2002) Cancer Cell 2, 243–247.
[18] van de Wetering, M. et al. (2003) EMBO Rep. 4, 609–615.
[19] Mizuguchi, H. and Kay, M.A. (1999) Hum. Gene Ther. 10, 2013–2017.
[20] Tahara-Hanaoka, S., Sudo, K., Ema, H., Miyoshi, H. and Nakauchi, H. (2002) Exp. Hematol. 30, 11–17.
[21] Miyoshi, H., Blomer, U., Takahashi, M., Gage, F.H. and Verma, I.M. (1998) J. Virol. 72, 8150–8157.
[22] Tontonoz, P., Hu, E., Graves, R.A., Budavari, A.I. and Spiegelman, B.M. (1994) Genes Dev. 8, 1224–1234.
[23] Gimble, J.M., Robinson, C.E., Wu, X., Kelly, K.A., Rodriguez, B.R., Kliewer, S.A., Lehmann, J.M. and Morris, D.C. (1996) Mol. Pharmacol. 50, 1087–1094.
[24] Baer, M., Nilsen, T.W., Costigan, C. and Altman, S. (1990) Nucleic Acids Res. 18, 97–103.
[25] Chawla, A., Schwarz, E.J., Dimaculangan, D.D. and Lazar, M.A. (1994) Endocrinology 135, 798–800.
[26] Kliewer, S.A., Forman, B.M., Blumberg, B., Ong, E.S., Borgmeyer, U., Mangelsdorf, D.J., Umesono, K. and Evans, R.M. (1994) Proc. Natl. Acad. Sci. USA 91, 7355–7359.
[27] Tontonoz, P., Hu, E. and Spiegelman, B.M. (1994) Cell 79, 1147–1156.
[28] Ramirez-Zacarias, J.L., Castro-Munozledo, F. and Kuri-Harcuch, W. (1992) Histochemistry 97, 493–497.
[29] Green, H. and Kehinde, O. (1975) Cell 5, 19–27.
[30] Wise, L.S. and Green, H. (1979) J. Biol. Chem. 254, 273–275.
[31] Doench, J.G., Petersen, C.P. and Sharp, P.A. (2003) Genes Dev. 17, 438–442.